

Supporting Information

Highly Efficient Palladium-Catalysed Carbon Dioxide Hydrosilylation Employing PMP Ligands

Patrick Steinhoff, Melanie Paul, Julian P. Schroers and Michael E. Tauchert*

Institute of Inorganic Chemistry, RWTH Aachen University, Landoltweg 1A, D-52074 Aachen, Germany

1	Experimental Procedures.....	2
2	Single Crystal X-ray diffraction.....	13
3	Overview of known complexes featuring a short Pd,M–distance	17
4	Computational Studies.....	17
5	Spectra.....	27
6	References.....	39

1 Experimental Procedures

1.1 General

1.1.1 Analytics

All manipulations were carried out in an MBraun glove box under an inert argon atmosphere. NMR-experiments were performed in Wilmad[®] quick pressure valve NMR tubes. ¹H, ¹¹B, ¹³C{¹H}, ¹⁹F{¹H}, and ³¹P{¹H} NMR spectra were recorded on a Bruker Avance II (400.1 MHz, probe: BBO) or a Bruker Avance (400.3 MHz, probe: ATM BBFO) spectrometer. ¹H and ¹³C{¹H} NMR spectra were referenced to residual solvent resonances.¹

Table S1. Shifts of residual solvent resonances used to reference NMR spectra.

Solvent	¹ H-NMR Shift in ppm	³¹ C-NMR Shift in ppm
DCM-d ₂	5.32	53.84
Benzene-d ₆	7.16	128.06
THF-d ₈	1.72	67.21
	3.58	25.31
CDCl ₃	7.26	77.16

CHN combustion analysis were carried out on an Elementar EL device by Elementar Analysensysteme GmbH. Infrared spectra were recorded on an Avatar 360 FT-IR E.S.P. device by Nicolet. Mass spectra (HRMS) and SIMS spectra were obtained by a MAT 95 spectrometer (Finnigan).

1.1.2 Chemicals

Dicyclohexylphosphine was synthesised from bromocyclohexane following established procedures.^{2,3} Unless stated otherwise all chemicals were purchased from Aldrich, ABCR, TCI, Merck or Alfa Aesar and used with no further purification. Cyclopentadienyl sodium was synthesised by adding cyclopentadiene to elemental sodium and removing all volatiles in vacuo. 2-(aminomethyl)-pyridine was distilled and stored under an argon atmosphere over MS 4 Å prior to use. Dimethylphenylsilane was distilled, degassed employing the freeze-pump-thaw technique, and stored over MS 4 Å prior to use. CO₂ 4.5 was purchased from Air Products and was passed through a sicapent column prior to use.

1.1.3 Solvents

DCM-d₂ and benzene-d₆ were degassed employing the freeze-pump-thaw technique and stored over activated molecular sieves (4 Å). THF-d₈ was dried over activated molecular sieves (3 Å), distilled under an argon atmosphere and degassed employing the freeze-pump-thaw technique. Toluene, diethylether, dichloromethane, tetrahydrofurane, and pentane were dried by an

MBraun solvent purification system. Benzene, 1,4-dioxane, *n*-hexane and hexamethyl-disiloxane were dried over sodium and distilled under argon prior to use and stored over activated molecular sieves (4 Å). DMF was dried over molecular sieves (3 Å), distilled under an argon atmosphere and degassed using the freeze-pump-thaw technique. Methanol was dried over molecular sieves (3 Å) overnight prior to use.

1.2 Syntheses

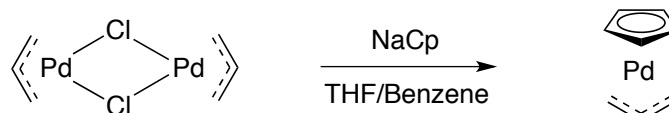
1.2.1 Allylpalladiumchloride dimer⁴



PdCl_2 (4.0 g, 23 mmol, 1 equiv.) and KCl (5.1 g, 68 mmol, 3 equiv.) was dissolved in H_2O (100 mL) and stirred for 1 h at room temperature. Allylchloride (5.6 mL, 69 mmol, 3 equiv.) was added and the reaction was heated to 50 °C and stirred for 18 h. The product was extracted from the aqueous phase using CHCl_3 . The combined organic phases were dried over MgSO_4 and volatiles were removed *in vacuo*. The product was obtained as a yellow solid (3.9 g, 22 mmol, 95%).

¹H NMR (CDCl_3 , 400.13 MHz): $\delta/\text{ppm} = 5.39$ (tt, $J = 12.1, 6.7$ Hz, 1H), 4.04 (dt, $J = 6.8, 0.7$ Hz, 2H), 2.97 (dt, $J = 12.1, 0.7$ Hz, 2H).

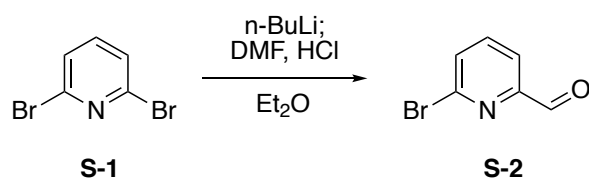
1.2.2 Cyclopentadienyl allyl palladium⁵



$[\text{CIPd}(\text{C}_3\text{H}_5)]_2$ (4.0 g, 11 mmol, 1 equiv.) was dissolved in a mixture of benzene (50 mL) and THF (50 mL). A solution of NaCp (2.9 g, 24 mmol, 2.2 equiv.) in THF (20 mL) was slowly added at -10 °C. The solution was stirred for 2 h maintaining a temperature between -8 °C and -2 °C. Volatiles were removed *in vacuo* at 0 °C. The residue was extracted with hexane (40 mL). The extract was filtered through celite and the solvent removed *in vacuo* at 0 °C. The product was obtained as a red solid (4.3 g, 20 mmol, 92%).

¹H NMR (C_6D_6 , 400.13 MHz): $\delta/\text{ppm} = 5.86$ (s, 5H), 4.59 (tt, $J = 10.8, 6.1$ Hz, 1H), 3.41 (d, $J = 6.1$ Hz, 2H), 2.10 (d, $J = 10.7$ Hz, 2H).

1.2.3 6-Bromo-2-pyridinecarboxyaldehyde S-2



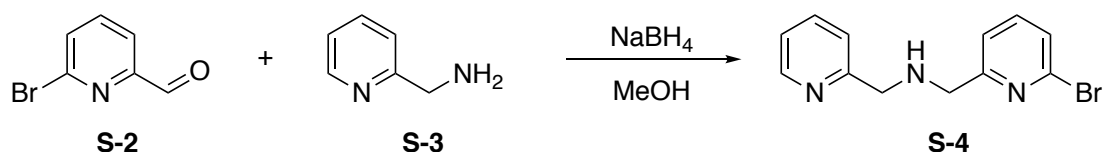
2,6-Dibromopyridine **S-1** (30.0 g, 127 mmol, 1.00 equiv.) was dissolved in Et_2O (500 mL) and cooled to -78 °C. *n*-Buli in hexane (83.1 mL, 1.6 M, 131 mmol, 1.04 equiv.) was added slowly

(2 h). The reaction was stirred for 15 min at room temperature and then cooled back down to $-78\text{ }^{\circ}\text{C}$. DMF (12.0 mL, 155 mmol, 1.22 equiv.) was added quickly. The mixture was stirred at $-78\text{ }^{\circ}\text{C}$ for 2 h, then HCl (18 mL) was added and the solution was allowed to thaw to room temperature. Water was added until all solids were dissolved. The phases were separated, the aqueous phase was washed with Et_2O (3 x 40 mL), the combined organic phases were dried over MgSO_4 and concentrated. The product was obtained by crystallisation from Et_2O at $-35\text{ }^{\circ}\text{C}$ as a white solid (20.7 g, 111 mmol, 88 %).

$^1\text{H NMR}$ (CDCl_3 , 400 MHz): $\delta/\text{ppm} = 10.00$ (d, $J = 0.7$ Hz, 1H), 7.93 (dd, $J = 6.7, 1.7$ Hz, 1H), 7.80 – 7.67 (m, 2H). $^{13}\text{C NMR}$ (CDCl_3 , 100.62 MHz): $\delta/\text{ppm} = 191.5$ (s, 1C), 153.4 (s, 1C), 142.5 (s, 1C), 139.4 (s, 1C), 132.6 (s, 1C), 120.3 (s, 1C).

The NMR data corresponds to those reported in literature.⁶

1.2.4 [(6-Bromo-2-pyridyl)methyl](2-pyridyl)methylamine

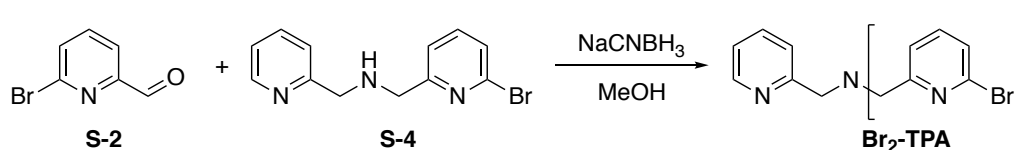


Amine **S-3** (6.12 g, 56.6 mmol, 1 equiv.) was slowly added to a solution of aldehyde **S-2** (10.5 g, 56.6 mmol, 1 equiv.) in methanol (140 mL). The solution was stirred for 1.5 h at room temperature and then cooled to $0\text{ }^{\circ}\text{C}$. A solution of NaBH_4 (2.15 g, 56.7 mmol, 1 equiv.) in methanol (40 mL) was added dropwise and the reaction mixture was stirred overnight at room temperature. By addition of aqueous HCl ($c = 1\text{ mol/L}$) the mixture was acidified to pH 1. The mixture was extracted with CHCl_3 (3x 80 mL). NaOH ($c = 1\text{ mol/L}$) was added to the aqueous phase until pH 8 was reached. The aqueous phase was again extracted with CHCl_3 (3x 80 mL). The combined organic phases were dried over MgSO_4 and concentrated *in vacuo*. The resulting solid was washed with acetone (3x 10 mL) and the product was obtained as a white solid after drying *in vacuo* (9.44 g, 33.9 mmol, 60%).

$^1\text{H NMR}$ (CDCl_3 , 400.13 MHz): $\delta/\text{ppm} = 8.55$ (ddd, $J = 4.9, 1.8, 1.0$ Hz, 1H), 7.64 (td, $J = 7.7, 1.8$ Hz, 1H), 7.50 (t, $J = 7.7$ Hz, 1H), 7.38 – 7.31 (m, 3H), 7.18 – 7.13 (m, 1H), 3.95 (s, 2H), 3.95 (s, 2H). $^{13}\text{C NMR}$ (CDCl_3 , 100.62 MHz): $\delta/\text{ppm} = 161.5$ (s, 1C), 159.3 (s, 1C), 149.3 (s, 1C), 141.6 (s, 1C), 138.7 (s, 1C), 136.4 (s, 1C), 126.2 (s, 1C), 122.2 (s, 1C), 122.0 (s, 1C), 120.9 (s, 1C), 54.5 (s, 1C), 54.1 (s, 1C).

The NMR data corresponds to those reported in literature.⁷

1.2.5 Bis[(6-bromo-2-pyridyl)methyl][(2-pyridyl)methyl]amine (**Br₂-TPA**)



AcOH (7.5 mL, 0.13 mol, 3 equiv.) was added to a solution of aldehyde **S-2** (8.9 g, 47 mmol, 1.1 equiv.) and amine **S-4** (12 g, 43 mmol, 1 equiv.) in MeOH (200 mL). The mixture was cooled to $0\text{ }^{\circ}\text{C}$ and stirred for 1 h. A solution of NaCNBH_3 (3.0 g, 48 mmol, 1.1 equiv.) in MeOH (40 mL) was added slowly and the solution was stirred for 72 h at room temperature.

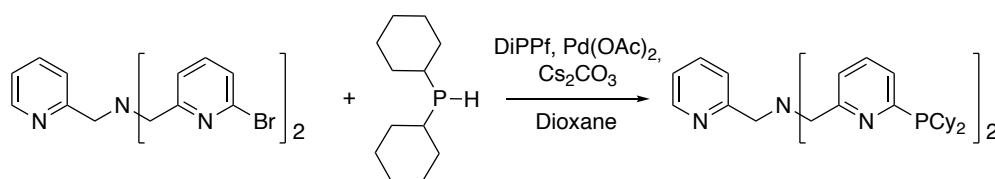
The solution was acidified to pH 1 with 1M HCl and all volatiles were removed *in vacuo*. The residue was solved in H₂O and extracted with CHCl₃ (3x 150 mL). The combined organic layers were dried over MgSO₄ and all volatiles were removed under reduced pressure. Pure **Br₂-TPA** was obtained as a white solid by crystallisation from Et₂O at -35 °C (15 g, 34 mmol, 78%).

¹H NMR (CDCl₃, 400.13 MHz): δ 8.54 (ddd, *J* = 4.9, 1.8, 0.9 Hz, 1H), 7.67 (td, *J* = 7.7, 1.8 Hz, 1H), 7.60 – 7.46 (m, 5H), 7.33 (dd, *J* = 7.6, 1.2 Hz, 2H), 7.17 (ddd, *J* = 7.5, 4.9, 1.2 Hz, 1H), 3.90 (s, 2H), 3.88 (s, 4H). ¹³C NMR (CDCl₃, 100.62 MHz): δ/ppm = 161.0 (s, 2C), 158.93 (s, 1C), 149.3 (s, 1C), 141.5 (s, 2C), 138.9 (s, 2C), 136.6 (s, 1C), 126.4 (s, 2C), 123.2 (s, 1C), 122.3 (s, 1C), 121.8 (s, 2C), 60.2 (s, 1C), 59.5 (s, 2C).

The NMR data corresponds to those reported in literature.⁸

1.2.6 Bis[(6-dicyclohexylphosphino-2-pyridyl)methyl][(2-pyridyl)methyl]amine

(DCPTPA)



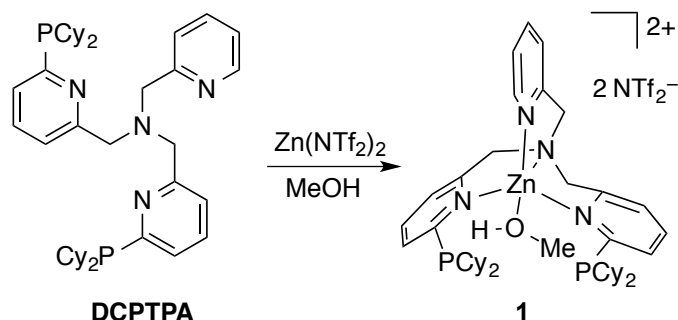
Br₂-TPA

DCPTPA

Br₂-TPA (3.0 g, 6.7 mmol, 1.0 equiv.), Pd(OAc)₂ (30 mg, 0.10 mmol, 0.02 equiv.), DiPPf (56 mg, 0.10 mmol, 0.02 equiv.) and CsCO₃ (4.8 g, 14 mmol, 2.2 equiv.) were stirred for 1 h in 1,4-dioxane (36 mL). Dicyclohexylphosphine (2.8 mL 14 mmol, 2.1 equiv.) was added and the solution was stirred for 18 h at 80 °C. Volatiles were removed *in vacuo*, the residue dissolved in DCM and filtered through a short pad of silica (0.04-0.063 mm). After removing all volatiles the resulting oil was stirred in hexane (10 mL) overnight. The resulting precipitate was filtered off and washed with hexane (3x 10 mL). After removing all volatiles *in vacuo* **DCPTPA** was obtained as an off white solid (3.8 g, 5.6 mmol, 83%).

¹H NMR (DCM-*d*₂, 400.13 MHz): δ/ppm = 8.41 (dt, *J* = 4.8, 1.4 Hz, 1H), 7.59 – 7.55 (m, 2H), 7.46 (td, *J* = 7.6, 1.9 Hz, 2H), 7.31 (dt, *J* = 7.8, 1.2 Hz, 2H), 7.25 (ddd, *J* = 7.5, 4.4, 1.2 Hz, 2H), 7.08 – 7.03 (m, 1H), 3.79 (d, *J* = 3.0 Hz, 6H), 2.03 (tq, *J* = 11.7, 3.0 Hz, 4H), 1.83 – 1.72 (m, 4H), 1.66 (dtt, *J* = 12.3, 3.3, 1.7 Hz, 4H), 1.56 – 1.44 (m, 12H), 1.29 – 0.84 (m, 20H). ³¹P NMR (DCM-*d*₂, 162.04 MHz): δ/ppm = 5.61 (s). ¹³C NMR (DCM-*d*₂, 100.62 MHz): δ/ppm = 161.6 (pd, *J* = 11.7 Hz, 2C, Cy-C), 160.6 (s, 1C, Cy-C), 160.0 (s, 2C, Cy-C), 149.4 (s, 1C, Cy-C), 136.7 (s, 1C, Cy-C), 135.3 (pd, *J* = 8.4 Hz, 2C, Py-C), 129.6 (pd, *J* = 33.2 Hz, 2C, Py-C), 123.3 (s, 1C, Py-C), 122.4 (s, 2C, Py-C), 122.3 (s, 1C, Py-C), 60.5 (s, 2C, CH₂), 60.3 (s, 1C, CH₂), 33.3 (s, 2C, Cy-C), 33.1 (s, 2C, Cy-C), 30.3 (s, 2C, Cy-C), 30.2 (s, 2C, Cy-C), 29.9 (s, 2C, Cy-C), 29.8 (s, 2C, Cy-C), 27.7 (s, 2C, Cy-C), 27.6 (s, 2C, Cy-C), 27.5 (s, 2C, Cy-C), 27.4 (s, 2C, Cy-C), 26.9 (s, 4C, Cy-C). **Elemental Analysis** calc. for C₄₂H₆₀N₄P₂: C: 73.87 H: 8.86 N: 8.20, found: C: 74.11% H: 8.89% N: 8.62%. **IR** (KBr): ν/cm⁻¹ = 3042 (vw), 3003 (vw), 2918 (vs), 2840 (s), 2369 (vw), 2345 (vw), 1590 (w), 1579 (m), 1559 (m), 1466 (vw), 1443 (s), 1353 (vw), 1341 (vw), 1291 (vw), 1264 (vw), 1264 (w), 1162 (w), 1112 (w), 1081 (vw), 1042 (vw), 983 (w), 890 (w), 855 (w), 804 (m), 750 (m), 649 (vw), 602 (vw), 524 (vw), 489,5 (w). **MS**: EI⁺ m/z = 682.3 (M), 599.3 (M-Cy) 590.3 (M-C₆H₆N), 394.2 (M - (C₆H₆N)PCy₂), 345.2 (M), 289.2 ((C₆H₆N)PCy₂), 206.1 ((C₆H₆N)PCy), 149.1 (M), 93.1 (C₆H₆N), 83.1 (Cy). **HRMS**: m/z: [M] calculated 682.4332 found 682.4288 (6.53 ppm).

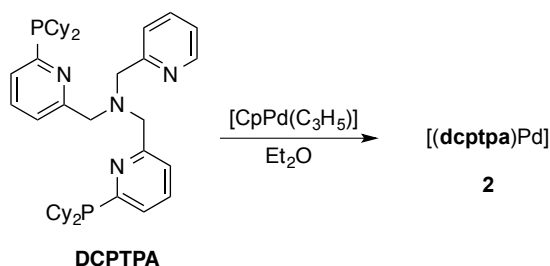
1.2.7 [(dcptpa)Zn](NTf₂)₂ **1**



Methanol was added to ligand **DCPTPA** (200.2 mg, 293.2 μmol , 1.0 equiv.) and $\text{Zn(NTf}_2)_2$ (182.9 mg, 292.3 μmol , 1.0 equiv.). The solution was stirred for 1 h at room temperature. All sediment was filtered off and the reaction solution was stored in the freezer. The formed crystals were filtered off. The product was obtained as a white solid after removing all volatiles in vacuo (110 mg, 82.1 μmol , 28%). The yield could be increased by further workup of the mother liquor (88.7 mg; 65.7 μmol , 23%, Overall Yield: 51%). Crystals suitable for XRD-analysis were obtained from cold MeOH (4 °C).

¹H NMR (DCM-*d*₂, 400.13 MHz): δ/ppm = 8.73 (dt, *J* = 5.3, 1.3 Hz, 1H), 8.25 – 8.05 (m, 3H), 7.86 (dd, *J* = 7.7, 1.0 Hz, 2H), 7.79 (ddd, *J* = 7.7, 5.4, 1.2 Hz, 1H), 7.74 (dq, *J* = 8.0, 1.3 Hz, 2H), 7.69 (dt, *J* = 7.9, 1.0 Hz, 1H), 4.51 (d, AB-resonance, *J* = 17.5 Hz, 2H), 4.44 (d, AB-resonance, *J* = 17.5 Hz, 2H), 4.29 (s, 2H), 3.42 (s, 3H, CH₃OH), 2.26 – 2.07 (m, 4H), 1.87 – 1.47 (m, 21H), 1.39 – 0.96 (m, 15H), 0.76 (tdq, *J* = 12.3, 9.3, 3.1 Hz, 2H). **³¹P NMR** (DCM-*d*₂, 162.04 MHz): δ/ppm = 32.14 (s, $\omega_{1/2}$ = 22 \pm 1 Hz). **¹³C NMR** (DCM-*d*₂, 100.62 MHz): δ/ppm = 159.63 (pt, *J* = 3.3 Hz, 2C, Py-C), 156.58 (pt, *J* = 8.3 Hz, 3C, Py-C), 149.23 (s, 1C Py-C), 143.46 (s, 1C, Py-C), 142.63 (s, 2C Py-C), 130.86 (s, 1C, Py-C), 127.22 (2C, Py-C), 127.12 (s, 1C, Py-C), 126.75 (s, 1C, Py-C), 120.39 (q, *J* = 321.5 Hz, 4C, CF₃), 57.51 (s, 2C, CH₂), 57.32 (s, 1C, CH₂), 51.13 (s, 1C, CH₃OH), 34.94 (pt, *J* = 2.6 Hz, 2C, Cy-C), 34.29 (pt, *J* = 3.3 Hz, 2C, Cy-C), 30.41 – 29.99 (pm, 6C, Cy-C), 29.82 (pt, *J* = 2.0 Hz, 2C, Cy-C), 27.46 – 27.22 (pm, 4C, Cy-C), 27.03 (pm, 4C, Cy-C), 26.25 (pd, *J* = 4.0 Hz, 4C, Cy-C). **¹⁹F{¹H} NMR** (377 MHz, DCM-*d*₂): δ/ppm = –79.38. **Elemental Analysis** calc. for C₄₆H₆₀F₁₂N₆O₈P₂S₄Zn • MeOH: C, 42.11%; H, 4.81%; N, 6.27%; found C, 41.61%; H, 4.897%; N, 6.26%. **IR** (KBr): ν/cm^{-1} = 2928 (s), 2854 (w), 1610 (vw), 1591 (vw), 1444 (w), 1354 (vs), 1335 (w), 1217 (s), 1192 (vs), 1138 (s), 1059 (s), 881 (vw), 852 (vw), 791 (w), 764 (vw), 741 (vw), 617 (s), 571 (s), 515 (s).

1.2.8 [(dcptpa)Pd] (**2**)

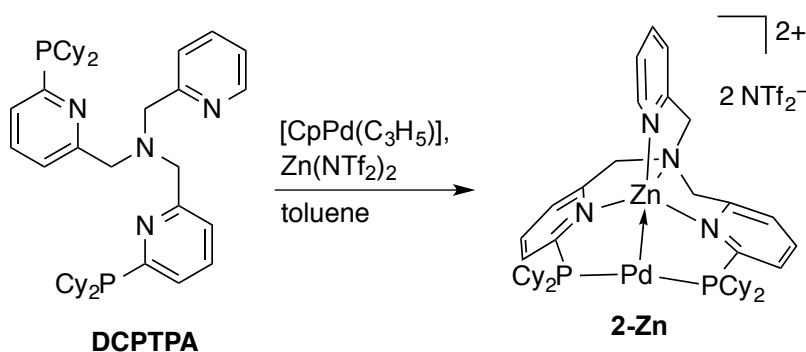


A solution of $[\text{CpPd}(\text{C}_3\text{H}_5)]$ (125.1 mg, 589.9 μmol , 1 equiv.) in Et₂O (10 mL) was slowly added to a solution of **DCPTPA** (400.0 mg, 585.7 μmol , 1 equiv.) in Et₂O (4 mL). The reaction was stirred for 2 h, during which a yellow precipitate was formed. The precipitate was isolated

by filtration, washed with ether (3x 4mL) and dried *in vacuo*. The product **1** was obtained as a yellow solid (413.8 mg, 524.2 μmol , 89.4%).

$^1\text{H NMR}$ (DCM- d_2 , 400.13 MHz): $\delta/\text{ppm} = 8.57 - 8.52$ (m, 0.12), 8.51 - 8.41 (m, 1.21), 7.81 - 6.90 (m, 12.33), 5.66 - 5.47 (m, 1.52), 4.24 - 3.72 (m, 8.33), 3.00 - 2.72 (m, 1.66), 2.56 - 0.82 (m, 73.47), 0.73 - 0.58 (m, 1.36). $^{31}\text{P NMR}$ (THF- d_8 , 162.04 MHz): $\delta/\text{ppm} = 44.52$ (s, 13.99), 40.71 (s, 2.41), 38.42 (s, 4.06), 37.93 - 35.03 (br. s, 11.15), 32.61 - 26.94 (br. s, 68.38). **IR** (KBr): $\nu/\text{cm}^{-1} = 3050$ (vw), 2930 (vs), 2850 (s), 2650 (vw), 1638 (w), 15801 (m), 1562 (m), 1560 (m), 1441 (w), 1340 (w), 1265 (w), 1209 (w), 1178 (w), 1161 (w), 1115 (w), 1084 (w), 1047 (vw), 1001 (w), 993 (w), 895 (w), 887 (w), 850 (w), 798 (w), 746 (m), 607 (w), 517 (w), 492 (w), 447 (w). **Elemental Analysis** calc. for $\text{C}_{42}\text{H}_{60}\text{N}_4\text{P}_2\text{Pd}$: C, 63.91%; H, 7.66%; N, 7.10%; found: C, 64.28%; H, 7.75%; N, 7.24%. **SIMS** (pos, NBA): $m/z = 705.2$ (100%), 788.2 (65%, M), 737.4 (65%), 804.2 (57%), 896.2 (49%), 591.2 (14%).

1.2.9 [(dcptpa)ZnPd](NTf₂)₂ (**2-Zn**)

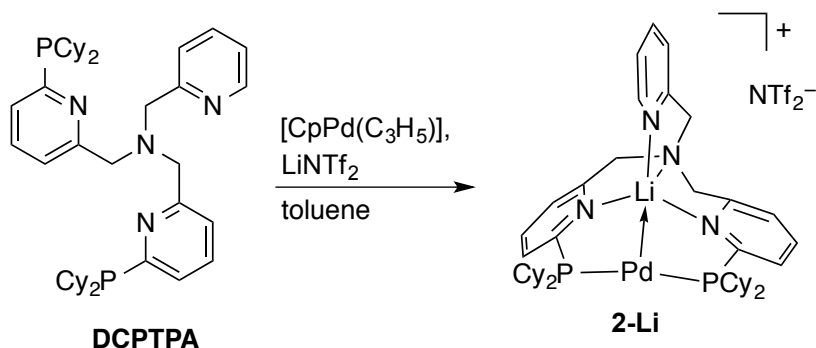


Ligand **DCPTPA** (200 mg, 293 μmol , 1.0 equiv.), $[\text{CpPd}(\text{C}_3\text{H}_5)]$ (62.3 mg, 293 μmol , 1.0 equiv.) and $\text{Zn}(\text{NTf}_2)_2$ (183 mg, 293 μmol , 1.0 equiv.) were weighted into a Schlenk tube equipped with a magnetic stirring bar. Toluene (6 mL) was added and the suspension was stirred for 2 h. The resulting 2 phases were separated by syringe and hexane (6 mL) was added to the lower phase. The solution was stirred overnight and the liquid was filtered off. After washing the solid with hexane and removing all volatiles *in vacuo* the product was obtained as a red-brown solid (252 mg, 178 μmol , 61%). Crystals suitable for XRD-analysis were obtained from a THF solution overlaid with HMDS.

$^1\text{H NMR}$ (400 MHz, THF- d_8): $\delta/\text{ppm} = 9.12$ (dd, $J = 5.4, 1.5$ Hz, 1H), 8.23 (t, $J = 7.7$ Hz, 2H), 8.14 (t d, $J = 7.8, 1.6$ Hz, 1H), 8.10 (d, $J = 7.6$ Hz, 2H), 7.81 (d, $J = 7.8$ Hz, 2H), 7.75 (dd, $J = 7.4, 5.3$ Hz, 1H), 7.71 (d, $J = 7.9$ Hz, 1H), 4.62 (d, AB-resonance, $J = 16.8$ Hz, 2H), 4.48 (d, AB-resonance, $J = 16.8$ Hz, 2H), 4.37 (s, 2H), 2.79 (ddt, $J = 11.6, 7.6, 3.8$ Hz, 2H), 2.24 (d, $J = 12.7$ Hz, 4H), 2.09 (d, $J = 12.9$ Hz, 2H), 1.99 - 0.82 (m, 44H, residual solvent signal of THF- d_8 included in integration). $^{13}\text{C}\{^1\text{H}\}$ NMR (101 MHz, THF- d_8): $\delta/\text{ppm} = 157.6$ (pt, $J = 7.0$ Hz, 2C, Py-C), 156.8 (s, 1C, Py-C), 155.9 (pt, 21.0 Hz, 2C, Py-C), 150.2 (s, 1C, Py-C), 142.7 (s, 1C, Py-C), 142.0 (s, 2C, Py-C), 130.2 (pt, $J = 3.1$ Hz, 2C, Py-C), 126.8 (s, 2C, Py-C), 126.0 (s, 1C, Py-C), 126.0 (s, 1C, Py-C), 120.9 (q, $J = 322.2$ Hz, 4C, CF₃), 58.6 (s, 3C, CH₂), 37.41 (pt, $J = 8.7$ Hz, 2C, Cy-C), 36.0 (pt, $J = 10.1$ Hz, 2C, Cy-C), 31.6 (br. s, 2C, Cy-C), 31.5 (pt, $J = 3.5$ Hz, 2C, Cy-C), 31.0 (pt, $J = 4.1$ Hz, 2C, Cy-C), 29.8 (s, 2C, Cy-C), 27.5-27.0 (pm, 8 C, Cy-C), 26.9 (s, 2C, Cy-C), 26.3 (s, 2C, Cy-C). $^{31}\text{P}\{^1\text{H}\}$ NMR (162 MHz, THF- d_8): $\delta/\text{ppm} = 58.12$ (s). $^{19}\text{F}\{^1\text{H}\}$ NMR (377 MHz, THF- d_8): $\delta/\text{ppm} = -79.69$ (s). **IR** (KBr): $\nu/\text{cm}^{-1} = 3086$ (vw), 2932 (vs), 2855 (s), 1612 (w), 1592 (m), 1567 (w), 1492 (w), 1449 (s), 1353 (vs), 1190 (vs),

1134 (vs), 1057 (vs), 1021 (m), 1002 (m), 885 (w), 788 (m), 739 (m), 652 (m), 616 (s), 600 (s), 570 (s), 509 (s). **Elemental Analysis** calc. for $C_{46}H_{60}F_{12}N_6O_8P_2PdS_4Zn \cdot THF$: C, 40.82%; H, 4.66%; N, 5.71%; found: C, 41.01%; H, 4.44%; N, 6.11%. **SIMS** (pos, NBA): $m/z = 1135.2$ (100%, $[MNTf_2]^+ - ^-NTf_2$), 761.0 (35%).

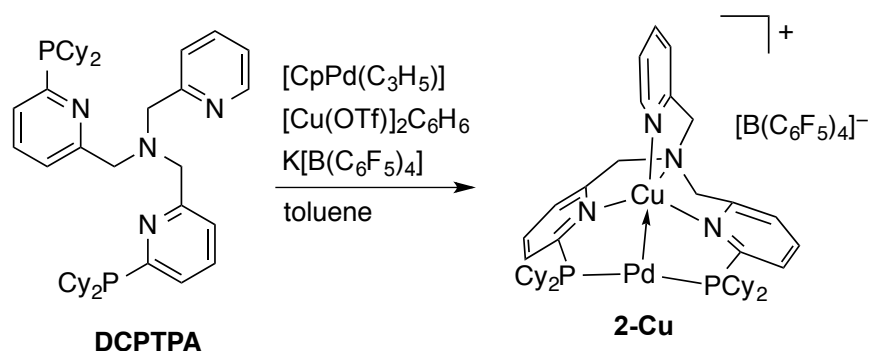
1.2.10 $[(dcptpa)LiPd]NTf_2$ (**2-Li**)



Ligand **DCPTPA** (500 mg, 732 μ mol, 1.0 equiv.), $[CpPd(C_3H_5)]$ (156 mg, 732 μ mol, 1.0 equiv.) and $Li(NTf_2)$ (210 mg, 732 μ mol, 1.0 equiv.) were weighted into a Schlenk tube equipped with a magnetic stirring bar. Toluene (6 mL) was added and the suspension was stirred for 2 h. The resulting two phases were separated by syringe and hexane (6 mL) was added to the lower phase. The solution was stirred overnight and the liquid was filtered off. After washing the solid with hexane and removing all volatiles in vacuo the product was obtained as a beige solid (582 mg, 541 μ mol, 74%). Crystals suitable for XRD-analysis were obtained from toluene overlaid with hexane.

1H NMR (400 MHz, C_6D_6): $\delta/ppm = 8.73$ (dd, $J = 5.3, 1.6$ Hz, 1H), 7.33 (t, $J = 7.7$ Hz, 2H), 7.19 (dt, $J = 7.7, 1.8$ Hz, 1H), 7.11 – 7.00 (m, 5H), 6.79 – 6.73 (m, 1H), 3.73 (d, AB-resonance $J = 16.2$ Hz, 2H), 3.67 (d, AB-resonance, $J = 15.4$ Hz, 2H), 3.66 (s, 2H), 2.27 – 2.04 (m, 4H), 2.00 – 1.17 (m, 30H), 1.14 – 0.68 (m, 10H). **$^{13}C\{^1H\}$ NMR** (101 MHz, C_6D_6): $\delta/ppm = 159.7$ (pt, $J = 8.0$ Hz, 2C, Py-C), 159.5 (s, 1C, Py-C), 159.2 (pt, $J = 21.1$ Hz, 2C, Py-C), 149.21 (s, 1C, Py-C), 138.1 (s, 1C, Py-C), 137.3 (s, 2C, Py-C), 126.3 (pt, $J = 3.6$ Hz, 2C, Py-C), 123.9 (s, 1C, Py-C), 123.8 (s, 2C, Py-C), 122.4 (s, 1C, Py-C), 121.2 (q, $J = 322.1$ Hz, 2C, CF_3), 58.6 (s, 2C, NCH_2), 58.4 (s, 1C, NCH_2), 36.9 (pt, $J = 7.1$ Hz, 2C, Cy-C), 33.5 (pt, $J = 8.8$ Hz, 2C, Cy-C), 31.6 (pt, $J = 4.6$ Hz, 2C, Cy-C), 30.9 (pt, $J = 3.8$ Hz, 2C, Cy-C), 30.7 (pt, $J = 5.9$ Hz, 2C, Cy-C), 29.4 (s, 2C, Cy-C), 27.2 – 26.9 (pm, 4C, Cy-C), 26.8 (s, 2C, Cy-C), 26.5 (pt, $J = 6.2$ Hz, 4C, Cy-C), 26.0 (s, 2C, Cy-C). **$^{31}P\{^1H\}$ NMR** (162 MHz, C_6D_6): $\delta/ppm = 39.75$ (s). **$^{19}F\{^1H\}$ NMR** (376.6 MHz, C_6D_6) $\delta/ppm = -78.35$ (s) ppm. **$^7Li\{^1H\}$ NMR** (155.5 MHz, C_6D_6): $\delta/ppm = 4.00$ (s, $\omega_{1/2} = 3 \pm 1$ Hz). **IR** (KBr): $\nu/cm^{-1} = 3058$ (vw), 2928 (vs), 2853 (s), 1599 (m), 1586 (m), 1556 (w), 1448 (s), 1355 (vs), 1227 (s), 1192 (vs), 1135 (vs), 1057 (vs), 1005 (m), 907 (w), 880 (w), 788 (m), 740 (m), 617 (m), 600 (m), 570 (m), 508 (m). **Elemental Analysis** calc. for $C_{44}H_{60}F_6LiN_5O_4P_2PdS_2 \cdot Toluene$: C, 52.42%; H, 5.87%; N, 5.99%; found: C, 52.51%; H, 6.10%; N, 6.44%. **SIMS** (pos, NBA): $m/z = 796.2$ (100%, $M^+ - ^-NTf_2$), 722.2 (47%), 706.1 (43%), 992.4 (17%).

1.2.11 [(dcptpa)CuPd][B(C₆F₅)₄] (2-Cu)



Ligand **DCPTPA** (200 mg, 293 μmol , 1.0 equiv.), $[\text{Cu}(\text{OTf})_2] \cdot \text{C}_6\text{H}_6$ (73.7 mg, 146 μmol , 0.5 equiv.) and $\text{K}[\text{B}(\text{C}_6\text{F}_5)_4]$ (210 mg, 292 μmol , 1.0 equiv) were weighted into a Schlenk flask. Benzene (60 mL) and a solution of $[\text{CpPd}(\text{C}_3\text{H}_5)]$ (62.8 mg, 294 μmol , 1 equiv.) in benzene (5 mL) were added. The reaction was stirred overnight, the precipitate was filtered off and all volatiles were removed from the filtrate *in vacuo*. The residue was stirred in hexane (20 mL) overnight, filtered off and the resulting solid washed with hexane (3x 15 mL). The product was obtained after removing all volatiles *in vacuo* as a brown powder (185 mg, 121 μmol , 42%).

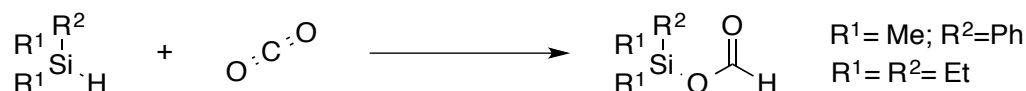
¹H NMR (600 MHz, THF-*d*₈) δ/ppm = 8.88 (d, J = 4.9 Hz, 1H), 7.81 – 7.76 (m, 3H), 7.63 (d, J = 7.6 Hz, 2H), 7.39 (d, J = 6.6 Hz, 1H), 7.34 (d, J = 7.8 Hz, 3H), 4.19 (d, AB- resonance, J = 15.8 Hz, 2H), 4.09 (d, AB- resonance, J = 15.8 Hz, 2H), 4.02 (s, 2H), 2.47 – 2.39 (m, 2H), 2.23 – 2.16 (m, 2H), 2.14 – 2.05 (m, 2H), 2.05 – 1.97 (m, 2H), 1.90 – 0.84 (m, 51H, residual solvent signal of THF-*d*₈ included in integration). **¹³C{¹H} NMR** (151 MHz, THF-*d*₈) δ/ppm = 159.2 (pt, J = 22.0 Hz, 2C, Py-C), 158.1 (pt, J = 7.1 Hz, 2C, Py-C), 158.1 (s, 1C, Py-C), 150.8 (s, 1C, Py-C), 149.3 (d, J = 242.5 Hz, 8C, B(C₆F₅)₄), 139.2 (d, J = 245.1 Hz, 4C, B(C₆F₅)₄), 138.2 (s, 1C, Py-C), 137.2 (d, J = 247.8 Hz, 8C, B(C₆F₅)₄), 137.1 (s, 2C), 128.6 (pt, J = 4.0 Hz, 2C, Py-C), 124.9 (s, 2C, Py-C), 124.9 (s, 1C, Py-C), 124.8 (s, 1C, Py-C), 59.6 (s, 2C, CH₂), 59.1 (s, 1C, CH₂), 38.5 (pt, J = 6.7 Hz, 2C, Cy-C), 35.3 (pt, J = 7.8 Hz, 2C, Cy-C), 32.4 (pt, J = 4.2 Hz, 2C, Cy-C), 31.9 (pt, J = 3.9 Hz, 2C, Cy-C), 31.5 (pt, J = 6.3 Hz, 2C, Cy-C), 31.1 (s, 2C, Cy-C), 28.2 (pt, J = 4.9 Hz, 2C, Cy-C), 28.1 (pt, J = 6.5 Hz, 2C, Cy-C), 27.6 (s, 2C, Cy-C), 27.4 (pt, J = 5.4, 4C, Cy-C Hz), 27.0 (s, 2C, Cy-C) (quaternary carbon of B(C₆F₅)₄ not observed). **³¹P{¹H} NMR** (162 MHz, THF-*d*₈): δ/ppm = 45.8 (s). **¹⁹F{¹H} NMR** (377 MHz, THF-*d*₈): δ/ppm = -132.73 (s, 2F), -165.15 (tr, J = 21.1 Hz, 1F), -168.61 (tr, J = 18.4 Hz, 2F). **¹¹B{¹H} NMR** (128 MHz, THF-*d*₈): δ/ppm = -18.4 ($\omega_{1/2}$ = 30 Hz). **IR** (KBr): ν/cm^{-1} = 2925 (s), 2848 (w), 2365 (vw), 2330 (vw), 1555 (w), 1509 (s), 1462 (vs), 1380 (vw), 1267 (w), 1240 (w), 1178 (vw), 1158 (vw), 1081 (w), 983 (s), 909 (vw), 882 (vw), 847 (vw), 773 (w), 754 (w), 684 (w), 660 (w), 575 (vw), 501 (vw). **SIMS** (pos, NBA): m/z = 853.4 (100%, M⁺ - NTf₂), 777.4 (60%), 761.4 (30%), 472.2 (25%), 260.1 (58%), 81.2 (32%). **SIMS** (neg, NBA): m/z = 678.5 (100%, B(C₆F₅)⁻), 166.9 (25 %, (C₆F₅)⁻).

1.3 Catalysis

1.3.1 Condition screening for hydrosilylation

Conditions were varied as described below. In all reactions a pressure of 1 bar CO₂ was used either stationary or dynamic. All reactions were terminated by removing the CO₂ atmosphere after the indicated time period.

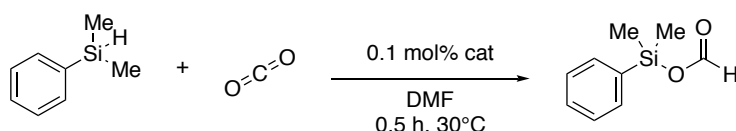
Table S2. Optimizing conditions for carbon dioxide hydrosilylation using **2-Zn** as catalyst.



#	solvent	silane	catalyst	mol %	time [h]	vessel	yield [%] ^h
1	THF ^a	PhMe ₂ SiH	2-Zn CsOPiv	1 1	0.5	NMR	33 ^{e,f}
2	THF ^a	PhMe ₂ SiH	2-Zn CsOPiv	0.5 1	0.5	NMR	33 ^{e,f}
3	THF ^a	PhMe ₂ SiH	2-Zn CsOPiv	0.1 1.0	0.5	NMR	19 ^{e,f}
5	THF ^b	Et ₃ SiH	2-Zn CsOPiv	1 1.0	0.5	NMR	0 ^e
6	THF ^d	PhMe ₂ SiH	2-Zn CsOPiv	1 1.0	0.5	NMR	25 ^{e,f}
4	THF ^a	PhMe ₂ SiH	2-Zn CsOPiv	1 1.0	0.5	25 mL Schlenk	100 ^g
7	DMF ^d	PhMe ₂ SiH	2-Zn CsOPiv	0.1 1.0	0.5	25 mL Schlenk	100 ^g
8	DMF ^d	PhMe ₂ SiH	2-Zn CsOPiv	0.05 0.5	0.5	25 mL Schlenk	64 ^g
9	DMF ^d	PhMe ₂ SiH	2-Zn CsOPiv	0.01 0.1	0.5	25 mL Schlenk	12 ^g

a) 0.4 mL THF; 0.1 mL PhMe₂SiH, b) 0.3 mL THF, 0.2 mL Et₃SiH; c) 0.3 mL THF, 0.2 mL PhMe₂SiH, d) 0.2 mL DMF; 0.5 mL PhMe₂SiH, e) stationary CO₂ atmosphere, once reaction vessel was pressurised no new CO₂ was added. f) Insufficient CO₂ volume in NMR tube for complete conversion. g) Constant CO₂ pressure open valve to CO₂ supply during reaction. h) determined by NMR.

1.3.2 General procedure for catalytic reaction



A 25 mL Schlenk tube equipped with a magnetic stirring bar was charged with the catalyst (3.3 μmol, 0.001 equiv.) and CsOPiv (7.6 mg, 0.033 mmol, 0.01 equiv.). DMF (0.2 mL) and, subsequently, PhMe₂SiH (0.50 mL, 3.3 mmol, 1 equiv.) were added. The argon atmosphere was removed using the pump-freeze thaw technique (3x). The reaction mixture was heated to 30 °C. The Schlenk tube was pressurised with CO₂ (1 bar) and stirred at 30 °C for 30 min. To ensure constant CO₂ pressure the valve to the CO₂ supply was kept open during the reaction. The CO₂ atmosphere was removed by using pump freeze thaw (3x) and 0.40 mL of the reaction mixture was transferred to an NMR tube. 0.20 mL of a standard stock solution (DCM-d₂, C₆Me₆, c = 0.308 M, 0.062 mmol) were added to the aliquot. The yield was determined by ¹H

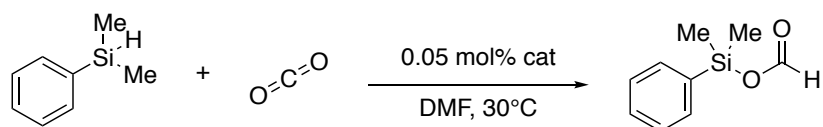
NMR spectroscopy by using the signals from the methyl-groups of product (0.59 ppm) and substrate (0.34 ppm).

Table S3. Hydrosilylation of carbon dioxide with PhSiMe₂H.

#	catalyst	m [mg]	n [μmol]	yield [%] ^a
1	2-Zn	4.6	3.3	100
2	2-Zn (no CsOPiv)	4.6	3.3	24
3	2-Li	3.5	3.3	9
4	2-Li LiNTf ₂	3.5 3.7	3.3 13	8
5	2-Cu	5.6	3.3	6
6	2	2.6	3.3	11
7 ^b	2 Zn(NTf ₂) ₂	2.6	3.3	57
		2.2	3.5	
8 ^b	DCPTPA Zn(NTf ₂) ₂	2.2	3.2	0
		2.2	3.5	
9 ^b	DCPTPA [CuOTf] ₂ · C ₆ H ₆	2.2 0.8	3.2 1.6	0.5

^aNMR yield against 1,2,3,4,5,6-hexamethylbenzene. ^b Stirred for 2h in DMF at r.t. before adding CsOPiv and PhMe₂SiH.

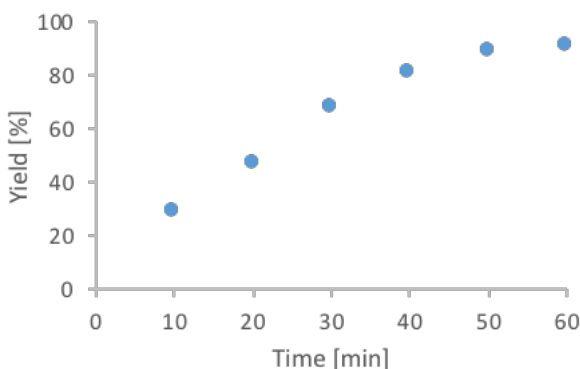
1.3.3 Time resolved monitoring of carbon dioxide hydrosilylation



A 25 mL Schlenk tube equipped with a stirring bar was charged with catalyst **2-Zn** (9.2 mg, 6.5 μmol, 0.0005 equiv.), CsOPiv (15 mg, 65 μmol, 0.005 equiv.) and C₆Me₆ (40 mg, 0.25 mmol, 0.02 equiv.) as internal NMR standard. DMF (0.8 mL) and Me₂PhSiH (2.00 mL, 13.0 mmol, 1 equiv.) were added and the argon atmosphere was removed using the freeze-pump-thaw technique (3x). The reaction mixture was heated to 30 °C and the Schlenk tube was pressurised with 1 bar CO₂ to start the reaction. To ensure constant CO₂ pressure the valve to the CO₂ supply was kept open during the reaction. The reaction was stirred at 30 °C and aliquots (0.2 mL) were taken every 10 min under CO₂ counter stream. The aliquots were diluted with 0.4 mL DCM-d₂ and the yield was determined by ¹H NMR spectroscopy using the signals from the SiMe₂ resonances of product (0.59 ppm) and substrate (0.34 ppm).

Table S4. Time resolved monitoring of carbon dioxide hydrosilylation.

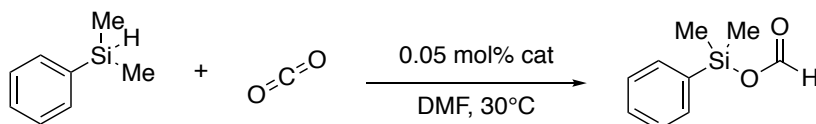
#	Time [min]	Yield [%] ^a
1	10	29
2	20	48
3	30	68
4	40	82
5	50	89
6	60	91



^aNMR yield against 1,2,3,4,5,6-hexamethylbenzene.

A polynomial trendline ($y = -0.0243x^2 + 2.987x$, $R^2 = 0.9971$) was fitted to the data points. The $TOF_{1/2}$ (turnover frequency at 50% conversion) was calculated from this equation as 3000 h^{-1} . Kinetic repeated with additional $\text{Zn}(\text{NTf}_2)_2$ (40.8 mg, 65 μmol , 0.005 equiv.) weighted into the Schlenk tube before adding DMF and silane. No conversion observed within 60 min monitoring in 10 min intervals.

1.3.4 Isolation of silyl formate $\text{PhMe}_2\text{SiOCHO}$



A 25 mL Schlenk tube equipped with a stirring bar was charged with catalyst **2-Zn** (9.2 mg, 6.5 μmol , 0.0005 equiv.), CsOPiv (15 mg, 65 μmol , 0.005 equiv.). DMF (0.8 mL) and Me_2PhSiH (2.0 mL, 13 mmol, 1 equiv.) were added and the argon atmosphere was removed using the freeze-pump-thaw technique (3x). The reaction mixture was heated to 30 °C and the Schlenk tube was pressurised with 1 bar CO_2 to start the reaction. To ensure constant CO_2 pressure the valve to the CO_2 supply was kept open during the reaction. After 60 minutes the reaction mixture was transferred to a 25 mL Schlenk flask and the product was distilled under reduced pressure (20 mbar, head temperature 90 to 98°C). The product was obtained as a colorless liquid (1.6 g, 9.2 mmol, 69%).

¹H NMR (400 MHz, DCM-d_2): $\delta/\text{ppm} = 8.13$ (s, 1H), 7.71 – 7.63 (m, 2H), 7.51 – 7.39 (m, 3H), 0.63 (s, 6H). ¹³C{¹H} NMR (101 MHz, DCM-d_2): $\delta/\text{ppm} = 161.1$ (1C, HCO_2), 135.4 (1C, Si–Ph), 133.9 (2C, Si–Ph), 130.8 (1C, Si–Ph), 128.4 (2C, Si–Ph), -1.4 (2C, Si–Me). ²⁹Si{¹H} NMR (80 MHz, DCM-d_2): $\delta/\text{ppm} = 14.0$ (s).

The NMR data corresponds to those reported in literature.⁹

1.3.5 Overview of established transition metal catalysts for CO₂

Table S5. Selected examples of transition metal catalysed hydrosilylation of carbon dioxide yielding silyl formates.^a

#	Catalyst	CO ₂ [bar]	additive	silane	t [h]	T [°C]	TON	TOF [h ⁻¹]	Ref
1	Cat-1	1	CsOPiv	PhMe ₂ SiH	1	25	19300	19300	10
2	Cat-2a	1	Cu(OAc) ₂ H ₂ O	PMHS	6	60	62000	10300	11
3	2-Zn	1	CsOPiv	PhMe ₂ SiH		30		3000	this work
4	Cat-2b	1	Cu(OAc) ₂ H ₂ O	PMHS	6	60	12000	2000	11
5	Cat-2c	1	Cu(OAc) ₂ H ₂ O	PMHS	6	60	8600	1400	11
6	[(IPr)Cu(OtBu)]	1	-	(EtO) ₃ SiH		60	7489	1248	12
7	Cat-3	5	-	nBuSiH ₃		RT	200	714	13
8	Ru ₂ Cl ₃ (MeCN) ₇	<i>b</i>	-	PhMe ₂ SiH	2	80	465	232	14
9	Cat-4	<i>c</i>	-	PhSiH ₃ or Ph ₂ SiH ₂	2	25	198	99	15
10	Rh ₂ (OAc) ₄	1	K ₂ CO ₃	PhMe ₂ SiH	2	50	180	90	16
11	RuCl ₃ (H ₂ O) _n	69-87	-	PhMe ₂ SiH	20	100	980	49	9
12	Cat-5	3	-	(Me ₃ SiO) ₂ MeSiH	144	90	88	0.6	17
13	[HRu ₃ (CO) ₁₁][N(PPh ₃) ₂]	50	-	Et ₃ SiH	24	60	292	12	18
14	Cat-6	6.8	-	(EtO) ₃ SiH	348.5	100	1006	2.9	19

^a Selection criteria: TON or TOF > 80. ^b 0.08 mol CO₂ in a 80 mL reactor charged with 30 mL of MeCN and 0.04 mol PhMe₂SiH. ^c 0.4 mol ¹³CO₂ in 3.5 mL NMR tube filled with 680 μL liquid volume.

2 Single Crystal X-ray diffraction

Crystal data, data collection parameters and refinement results for **1**, **2-Li** and **2-Zn** have been compiled in Table S6. Intensity data were collected on a Bruker D8 goniometer with APEX

CCD area detector in ω -scan mode using Mo-K α radiation ($\lambda = 0.71073 \text{ \AA}$) from an Incoatec microsource with multilayer optics. A temperature of 100(2) K was maintained with the help of an Oxford Cryostream 700 instrument. Data were collected with SMART,²⁰ integrated with SAINT²¹ and corrected for absorption by multi-scan methods with SADABS.²²

Using Olex2,²³ the structure was solved with the ShelXS structure solution program employing direct methods,²⁴ or with the olex2.solve structure solution program using charge flipping.²⁵ Full-matrix least-square refinements based on F^2 were performed with SHELXL.²⁴ Non-hydrogen atoms were assigned anisotropic displacement parameters unless stated otherwise. In case of **2-Li** the counter ion NTf₂ was found to be disordered and split on two positions. Additionally, one molecule of disordered toluene was observed in a late stage of refinement. 0.5 of the NTf₂-ion and 1 toluene was dealt with by application of the program SQUEEZE²⁶ as implemented in Platon.^{27, 28} The trispyridyl- unit and one cyclohexyl group in **2-Li** are disordered. Site occupancy refinement converged in a ratio of 0.25:0.75. The minor part and the NTf₂ anion have only been refined isotropically.

These data can be obtained free of charge from The Cambridge Crystallographic Data Centre via www.ccdc.cam.ac.uk/data_request/cif. The presentation of crystal structures was done with Mercury 3.9²⁹ or Platon.^{27, 28}

Table S6. Crystal data and structure refinement for **1**, **2-Zn** and **2-Li**.

Complex / CCDC	1 1855254	2-Zn · 1 THF 1569435	2-Li · 1 toluene 1815009
Empirical formula	C ₄₇ H ₆₄ F ₁₂ N ₆ O ₉ P ₂ S ₄ Zn	C ₅₀ H ₆₈ F ₁₂ N ₆ O ₉ P ₂ PdS ₄ Zn	C ₅₁ H ₆₈ F ₆ LiN ₅ O ₄ P ₂ PdS ₂
Formula weight	1340.59	1487.05	1872.59
Temperature/K	100(2)	100(2)	100(2)
Crystal system	Triclinic	Monoclinic	Monoclinic
Space group	P-1	P2 ₁ /n	C2/c
a/Å	13.7809(10)	15.0449(7)	14.6156(8)
b/Å	16.7029(12)	14.2330(7)	19.4178(10)
c/Å	26.20578(18)	29.2644(13)	40.0329(19)
α/°	87.1040(10)	90	90
β/°	89.9450(10)	94.5890(10)	99.0830(10)
γ/°	77.8480(10)	90	90
Volume/Å ³	5855.8(7)	6246.4(5)	11219.0(10)
Z	4	4	8
ρ _{calc} /cm ³	1.521	1.581	1.109
μ/mm ⁻¹	0.712	0.949	0.467
F(000)	2768.0	3040.0	3900.0
Crystal size/mm ³	0.21 x 0.18 x 0.16	0.23 × 0.17 × 0.14	0.19 × 0.18 × 0.16
2θ range /°	2.50 to 51.02	3.18 to 61.9	3.52 to 52.98
Index ranges	-16 ≤ h ≤ 16 -20 ≤ k ≤ 20 -31 ≤ l ≤ 31	-21 ≤ h ≤ 21 -20 ≤ k ≤ 17 -42 ≤ l ≤ 40	-18 ≤ h ≤ 18 -24 ≤ k ≤ 24 -50 ≤ l ≤ 50
Refls collected	66902	71133	68052
Independent reflections	21767 [R _{int} = 0.0794, R _{sigma} = 0.0915]	18553 [R _{int} = 0.0350, R _{sigma} = 0.0343]	1106 [R _{int} = 0.0509, R _{sigma} = 0.0387]
Data/restraints/parameters	21767/6/1467	18553/0/766	11606/70/578
GOF	1.046	1.020	1.039
Final R indexes [I>=2σ (I)]	R ₁ = 0.0466, wR ₂ = 0.0998	R ₁ = 0.0307, wR ₂ = 0.0717	R ₁ = 0.0784, wR ₂ = 0.1889
Final R indexes [all data]	R ₁ = 0.0725, wR ₂ = 0.1097	R ₁ = 0.0397, wR ₂ = 0.0756	R ₁ = 0.0907, wR ₂ = 0.1976
Largest diff. peak/hole / e Å ⁻³	0.47 / -0.40	0.59 / -0.57	4.10/-1.25
Structure solution program	ShelXS	Olex2.solve	ShelXS
SQUEEZE	n.a.	n.a.	Solvent accessible void: 2729 Å ³ Electron count voids: 1029 Good agreement (912 electrons) with anticipated 8 molecules of toluene and 8 x 0.5 molecules of NTf ₂ .
Comments	n.a.	n.a.	Remaining electron density of 4.10 located within disordered NTf ₂ -anion.

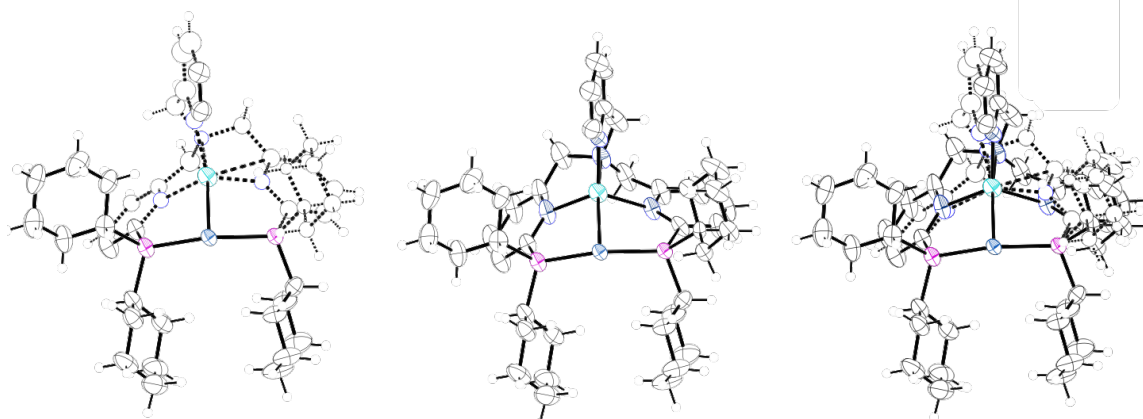


Fig. S1. Solid state structure of minor (25.5%, left) and major (74.5%, middle) conformer of **2-Li** (superposition: right). ORTEPs depicted at the 50% probability level. H atoms NTf₂-anion and solvent toluene have been omitted for clarity.

3 Overview of known complexes featuring a short Pd,M–distance

The Cambridge Crystallographic Data Centre (CCDC) was searched on August 5th 2018 for structures featuring a Pd–M (M = Li, Cu, Zn) bond. The found heterometallic complexes (3 x Pd/Li,^{30–32} 11 x Pd/Cu,^{33–42} 13 x Pd/Zn^{43–51}) are displayed in Fig. S2, provided that they contain less than 8 metallic centers.

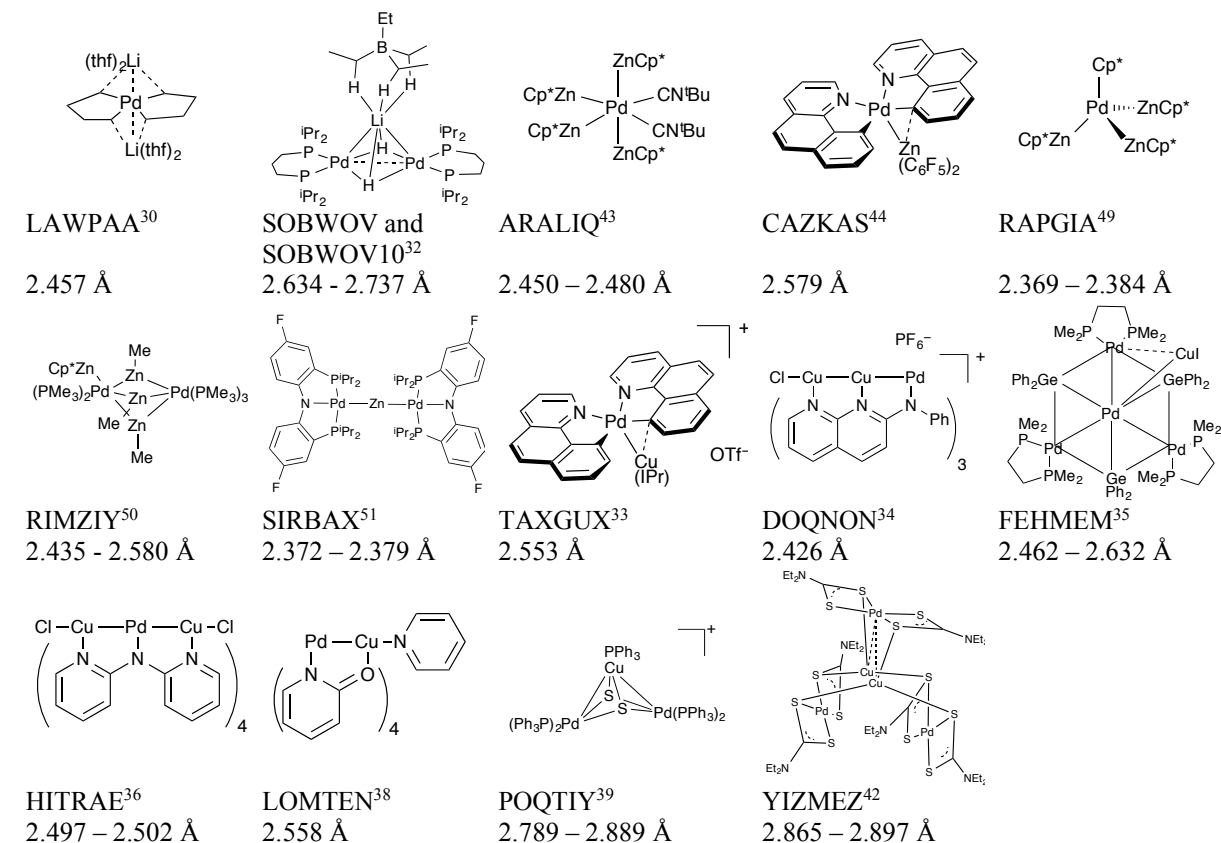


Fig. S2. Known palladium complexes featuring Li^I, Cu^I or Zn^{II} as metalloligand.

4 Computational Studies

4.1 Computational methods

Geometry optimisations were carried out without any symmetry restrictions. The minimum on the potential energy surface was confirmed by the absence of an imaginary frequency in the vibrational spectrum. Geometry optimisations and frequency analysis were performed using Turbomole 7.0.1.^{52, 53} The RI approximation⁵⁴ was used applied throughout. Calculations were performed with the BP86^{55, 56} functional, utilizing a def-SVP^{57, 58} basis set. Complexes **2-Zn** and **2-Li** were optimised using xyz-coordinates (excluding anion and solvent) from the solid-state structure. Complex **2-Cu** was optimised starting from xyz-coordinates of **2-Zn** with Zn(II) replaced by Cu(I). Complexes **3-Zn**, **3-Li** and **3-Cu** were optimised based on optimised structures of complexes of **2-Zn**, **2-Li** and **2-Cu** in which the PCy₂ groups had been dissipated to PMe₂ groups.

Electronic structures of complexes **3-Zn**, **3-Li** and **3-Cu** were studied using Natural Bond Orbital analysis (NBO-6 program)⁵⁹ implemented in the Gaussian 09 suite of programs.⁶⁰ NBO

and NLMO analyses were performed with the BP86 functional, utilizing 6-31G(d)^{61, 62} (H, Li, C, N), MWB10 (P),⁶³ MDF10⁶⁴ (Cu, Zn) and MWB28⁶³ (Pd) basis sets.

4.2 Comparison of optimised structures with solid state structures

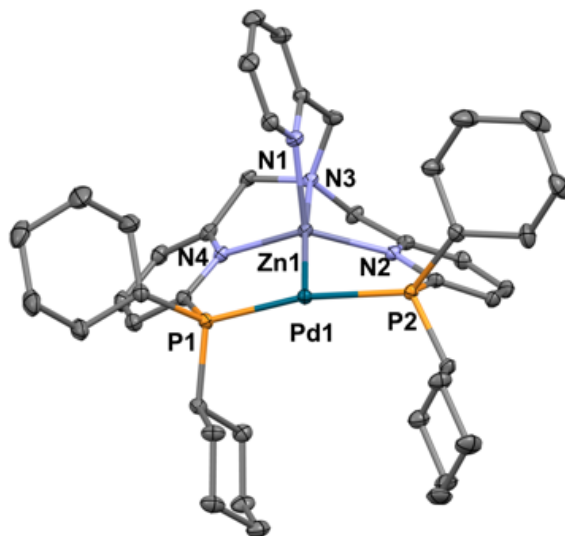


Table S7. Comparison of structural parameters of **2-Zn** (XRD), **2-Zn*** (DFT) and **3-Zn** (DFT).

Parameter	2-Zn (XRD)	2-Zn* (BP86/def-SVP)	3-Zn (BP86/def-SVP)
Zn,Pd	2.4652(2)	2.498	2.506
P1,Pd	2.2961(4)	2.334	2.313
P2,Pd	2.2888(4)	2.328	2.319
Zn,N1	2.0675(13)	2.127	2.099
Zn,N2	2.0826(13)	2.156	2.135
Zn,N3	2.2955(13)	2.304	2.288
Zn,N4	2.0963(13)	2.138	2.125
P1,Pd,P2	156.214(15)	165.4	166.0
N3,Zn,Pd	172.48(3)	163.8	165.9

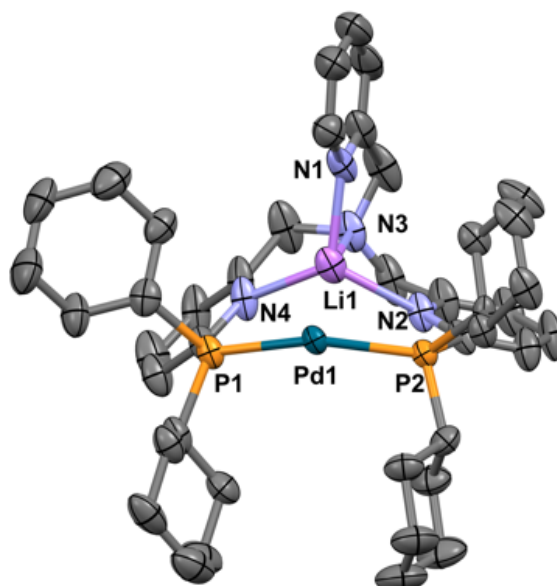


Table S8. Comparison of structural parameters of **2-Li** (XRD), **2-Li*** (DFT) and **3-Li** (DFT).

Parameter	2-Li (XRD)	2-Li* (BP86/def-SVP)	3-Li (BP86/def-SVP)
Li,Pd	2.665(9)	2.697	2.713
P1,Pd	2.2612(13)	2.303	2.290
P2,Pd	2.2705(13)	2.309	2.295
Li,N1	2.073(13)	2.171	2.119
Li,N2	2.124(13)	2.177	2.137
Li,N3	2.195(12)	2.219	2.217
Li,N4	2.103(11)	2.146	2.131
P1,Pd,P2	157.27(5)	165.2	166.0
N3,Li,Pd	162.6(6)	158.6	160.5

4.3 Natural Bond Orbital Analysis

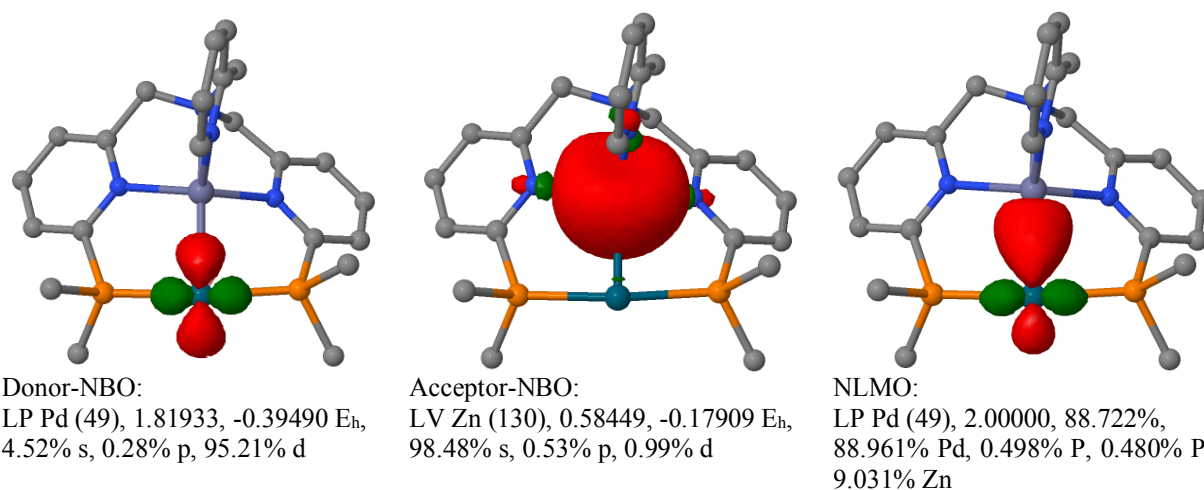


Fig. S3. NBO/NLMO plots **3-Zn**. NBO: orbital descriptor, occupancy, orbital energy, hybrid contributions. NLMO: orbital descriptor, occupancy, percentage of parent NBO, atomic contributions. E(2) of Pd–Zn bond from second order perturbation theory analysis of Fock matrix in NBO basis: 93.30 kcal/mol.

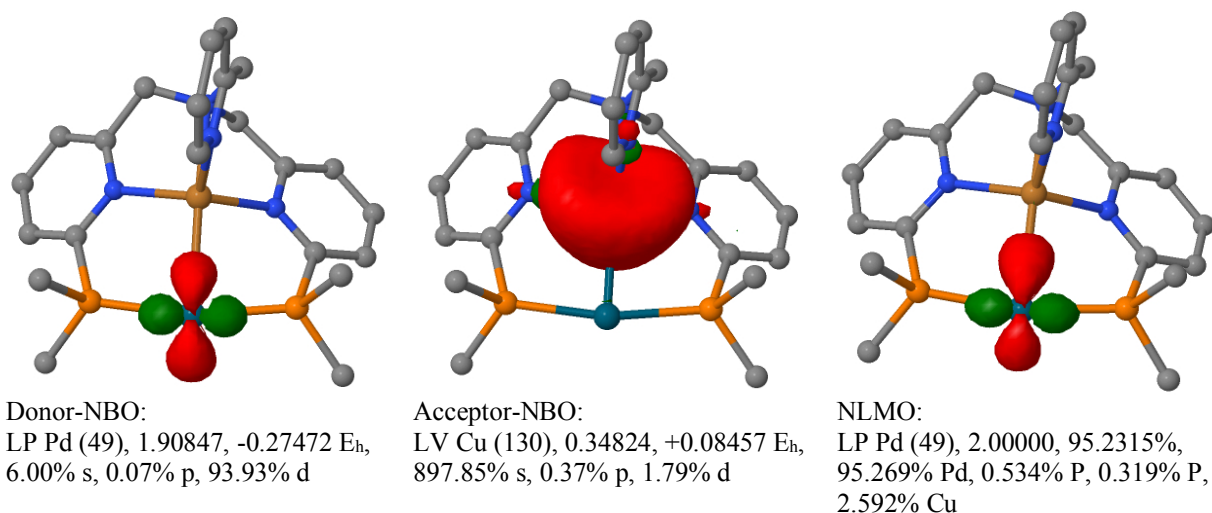


Fig. S4. NBO/NLMO plots **3-Cu**. NBO: orbital descriptor, occupancy, orbital energy, hybrid contributions. NLMO: orbital descriptor, occupancy, percentage of parent NBO, atomic contributions. E(2) of Pd–Cu bond from second order perturbation theory analysis of Fock matrix in NBO basis: 28.78 kcal/mol.

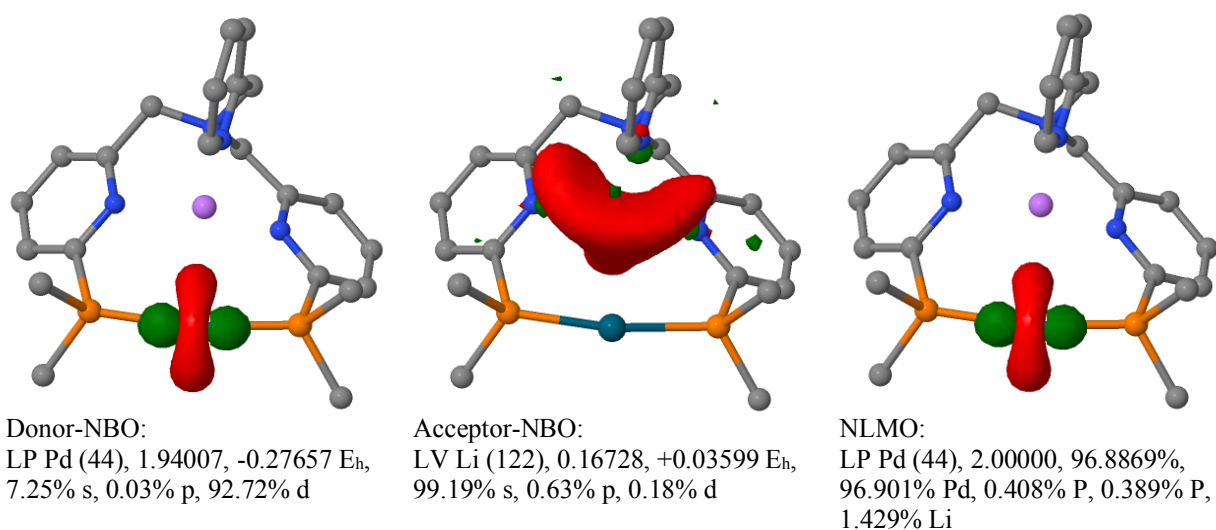


Fig. S5. NBO/NLMO plots **3-Li**. NBO: orbital descriptor, occupancy, orbital energy, hybrid contributions. NLMO: orbital descriptor, occupancy, percentage of parent NBO, atomic contributions. E(2) of Pd–Li bond from second order perturbation theory analysis of Fock matrix in NBO basis: 11.76 kcal/mol.

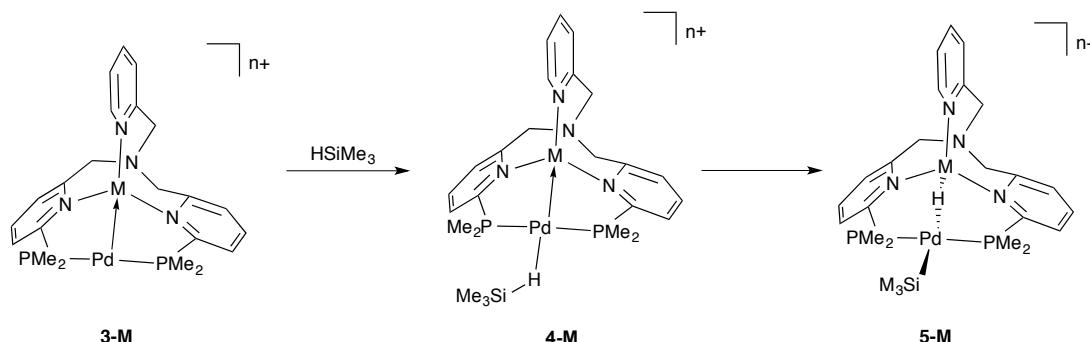
4.4 Interaction between complexes **3-M** with Me₃SiH

DFT calculations were performed to elucidate the effect of the Zn-ligand in palladium catalyzed CO₂ hydrosilylation. **DMPTPA** was used as a model ligand and Me₃SiH as a model substrate. Hydrosilylation of CO₂ with Me₃SiH gives an ΔE of -10.3 kcal/mol and an $\Delta G_{298.15K}$ of -0.2 kcal/mol using BP86/def-SV(P) for optimization

Two possible mechanistic pathways were considered:

- 1) Oxidative addition of the silane toward complex **3-M** via silane adduct formation (**4-M**) yielding **5-M** (Scheme S1)

- 2) Reaction of a Pd⁰-H complex **6-M** with CO₂ yielding formate complex **7-M** (**Scheme S2**). This mechanism has been suggested based on isolated Ni⁰-H and Ni⁰-OCHO intermediates by Lu and coworkers for CO₂ hydrogenation using a catalyst featuring a dative Ni⁰→Ga^{III} bond.⁶⁵



Scheme S1. Mechanistic route 1): Oxidative addition of silane towards **3-M**.

Route 1

The bond dissociation energy of the silane adducts **4-M** increases in the order of Li < Cu < Zn (**Error! Reference source not found.**). Similarly, the Pd,H distance decreases, and the Si,H distance increases in this order, suggesting that an increased acceptor strength of the metalloligand facilitates silane complexation and Si-H bond activation.

Table S9. Selected bond distances and bond dissociation energies of **4-M**.^a

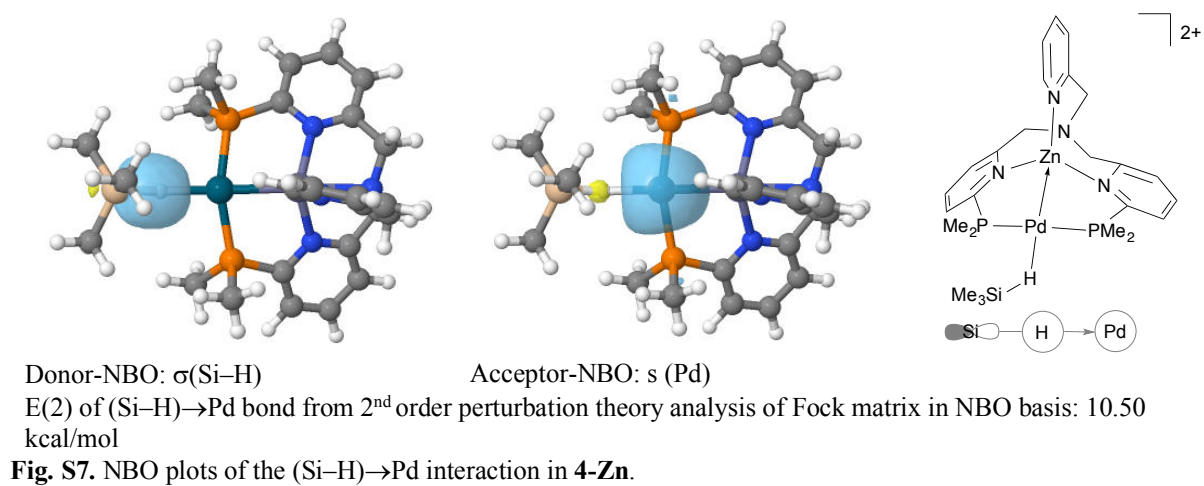
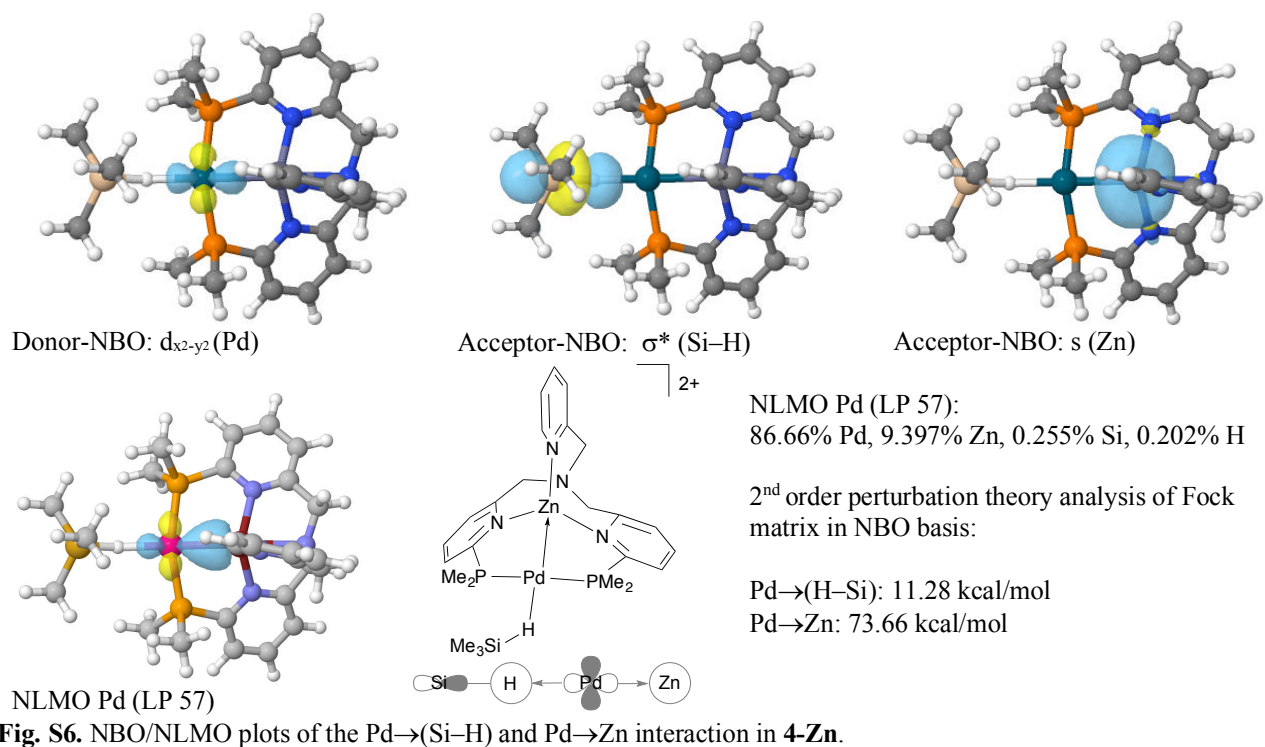
4-M	d(Si,H) [Å]	d(Pd,H) [Å]	d(Pd,M) [Å]	BDE ^b (Pd,H) [kcal/mol]
4-Zn	1.577	1.901	2.526	10.94
4-Cu	1.560	1.942	2.684	3.63
4-Li	1.558	1.942	2.818	2.64

^aTurbomole 7.0.1, BP86/SV(P). ^bBond dissociation energy.

NBO/NLMO calculations were performed on complexes **4-M** to elucidate the impact of the metalloligand on silane adduct formation (Fig. S6 - Fig. S11). The silane-palladium bond was composed in all cases of two donor-acceptor interactions.

Firstly, an occupied d_{x²-y²}-type palladium orbital, which also binds to the unoccupied s-type orbital of the metalloligand, interacts with the σ* (Si-H) bond of the silane. The NBO stabilizing energy of this palladium-silane interaction increases with the strength of the acceptor properties of the metalloligand (**4-Li**: 7.59 kcal/mol, **4-Cu**: 9.17 kcal/mol, **4-Zn**: 11.3 kcal/mol), which is in line with the observed Pd-H bond dissociation energies of **4-M** (Table S9).

Secondly, the σ (Si-H) bond interacts as a donor with an unoccupied s-type palladium acceptor orbital. This dative bond is not affected by the metalloligands.



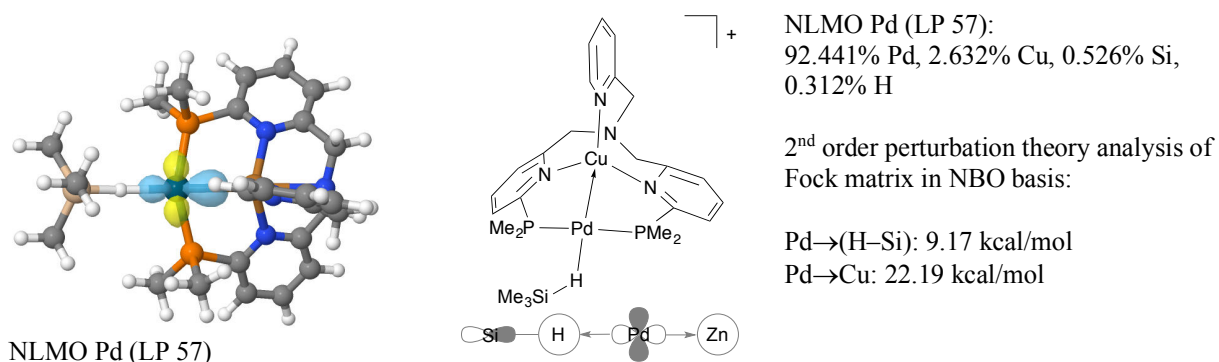
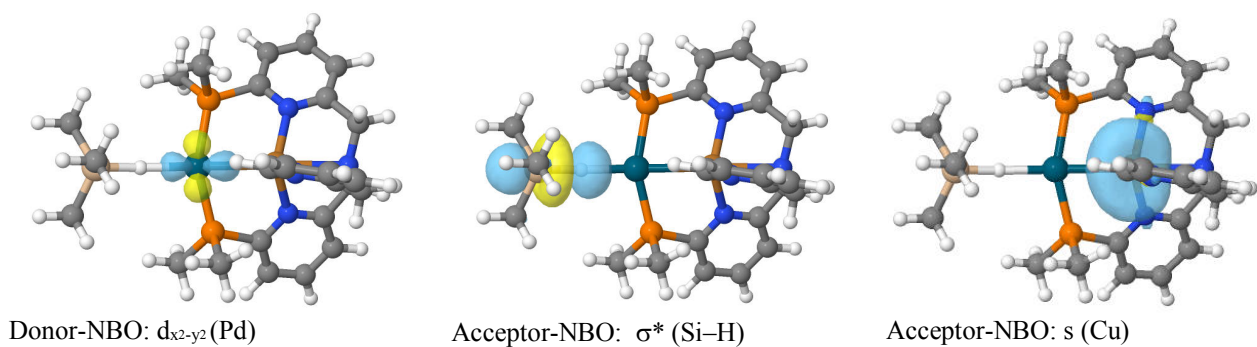


Fig. S8. NBO/NLMO plots of the Pd→(Si-H) and Pd→Cu interaction in **4-Cu**.

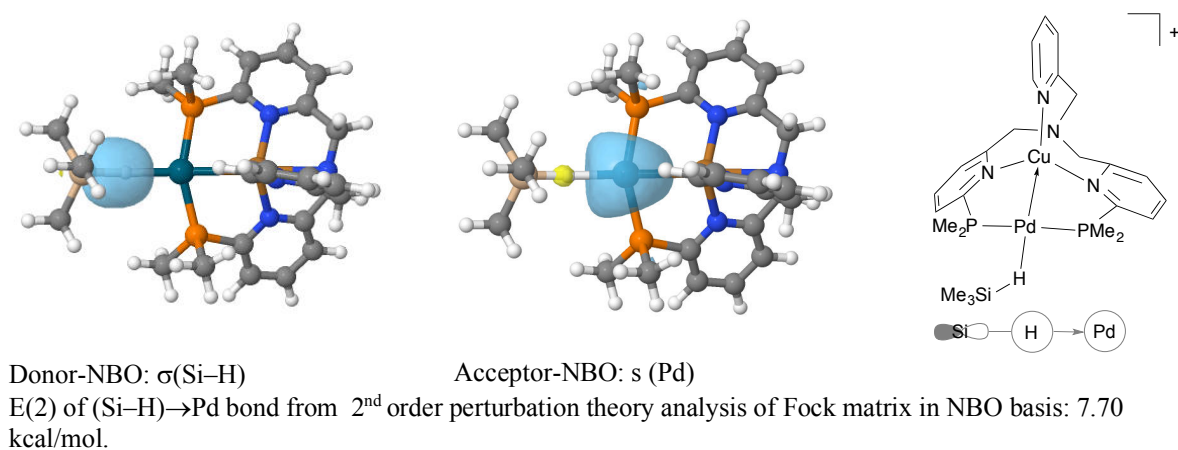


Fig. S9. NBO plots of the (Si-H)→Pd interaction in **4-Cu**.

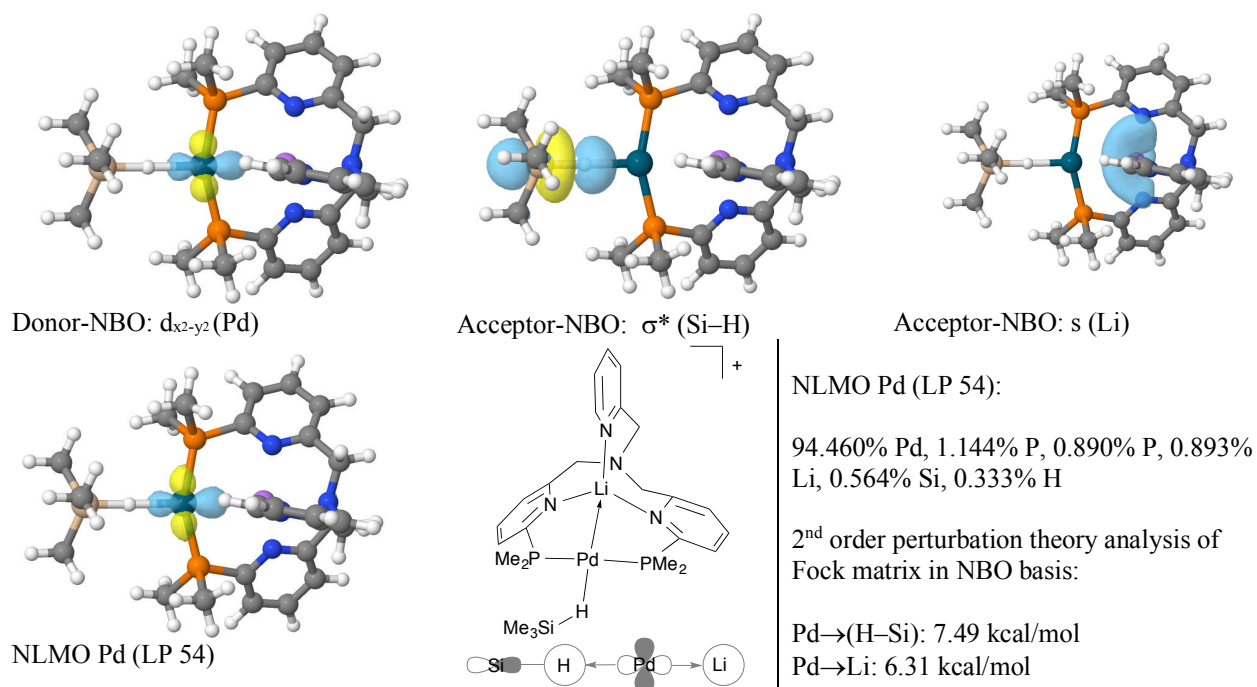


Fig. S10. NBO/NLMO plots of the Pd→(Si-H) and Pd→Li interaction in **4-Li**.

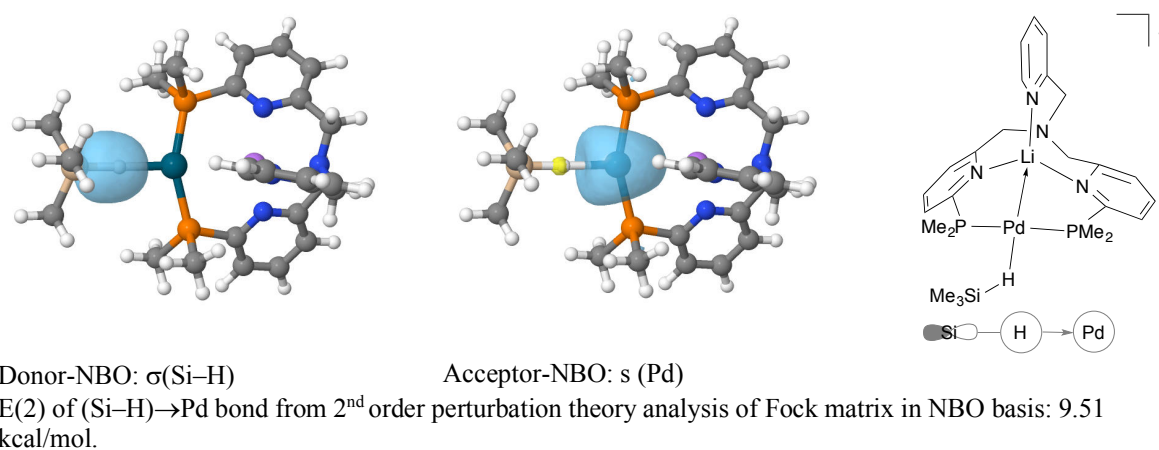


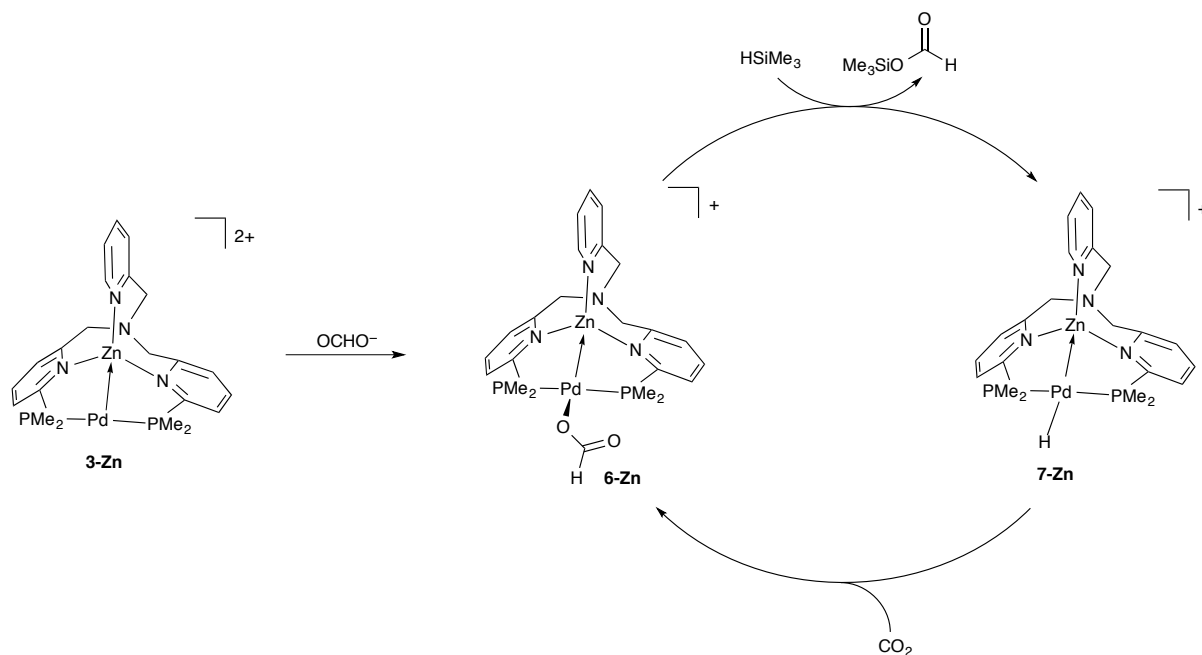
Fig. S11. NBO plots of the (Si-H)→Pd interaction in **4-Li**.

The oxidative cleavage of the Si-H bond in **4-Zn** gives **5-Zn**, in which the hydride adopts a bridging position between the two metals (Scheme S1). This transformation is an uphill process ($\Delta E = +19.8$ kcal/mol).

Route 2

As a starting point formate complex **6-Zn** was chosen. This is in line with the observation, that **3-Zn** readily reacts with CsOPiv, used as an additive in the hydrosilylation reactions. The formate ligand in **6-Zn** adopts a similar coordination position as the NTF₂-anion in the solid state structure of **3-Zn**. The reaction energy of this transformation was calculated as $\Delta E = -156.9$ kcal/mol ($\Delta G_{298.15} = -144.7$ kcal/mol) in the gas phase. According to the mechanism observed by Lu for her Ga/Ni system reaction with HSiMe₃ would then generate Pd⁰-hydride

7-Zn with simultaneous extrusion of silyl formate ($\Delta E = +7.8$ kcal/mol, $\Delta G_{298.15} = +5.0$ kcal/mol).⁶⁵ Insertion of CO₂ into the Pd–H bond then regenerates formate complex **6-Zn** ($\Delta E = -18.1$ kcal/mol, $\Delta G_{298.15} = -5.1$ kcal/mol) closing the catalytic cycle.



Scheme S2. Mechanistic route 2): Intermediate formation of Pd⁰–H (**7-M**).

In comparison, a ΔE value of +7.4 kcal/mol ($\Delta G_{298.15} = +6.6$ kcal/mol) was found for the transition of **6-Li** to **7-Li**. Regeneration of **6-Li** was calculated as $\Delta E = -17.7$ kcal/mol ($\Delta G_{298.15} = -6.9$ kcal/mol). The higher energetic position of hydride **7-M** relative to formate **6-M** with lithium as acceptor ligand compared to zinc could possibly explain the decreased reaction velocity of catalyst **2-Li** compared to **2-Zn**.

Possible stabilization of the palladium hydride intermediate **7-Zn** and **7-Li** by the metalloligand was examined by NBO/NLMO analysis (Fig. 12 and Fig. 13). For **7-Zn** NBO/NLMO analysis suggested that two s-type orbitals at Si and H each form a σ -Zn,H and σ^* -Zn,H bond. The unoccupied σ -Zn,H bond acts as an NBO-acceptor for an $d_{x^2-y^2}$ -type palladium NBO-donor with an associated NBO stabilizing energy of 90.3 kcal/mol. The corresponding palladium NLMO has significant contributions of both zinc (8.103%) and hydrogen (5.776%).

The NLMO of the σ^* -Zn,H bond was found occupied with two electrons, emphasizing that complex **7-Zn** is best described as a Pd⁰-hydride.

In contrast, no significant stabilization of the hydride by the lithium metalloligand was found in **7-Li**. Here, a Pd–H bond is observed, which interacts weakly with an s-type acceptor orbital at lithium (NBO stabilizing energy: 12.42 kcal/mol). Additionally, a weak Pd⁰→Li^I interaction, similar to the one in **3-Li**, is found (NBO stabilizing energy: 8.45 kcal/mol).

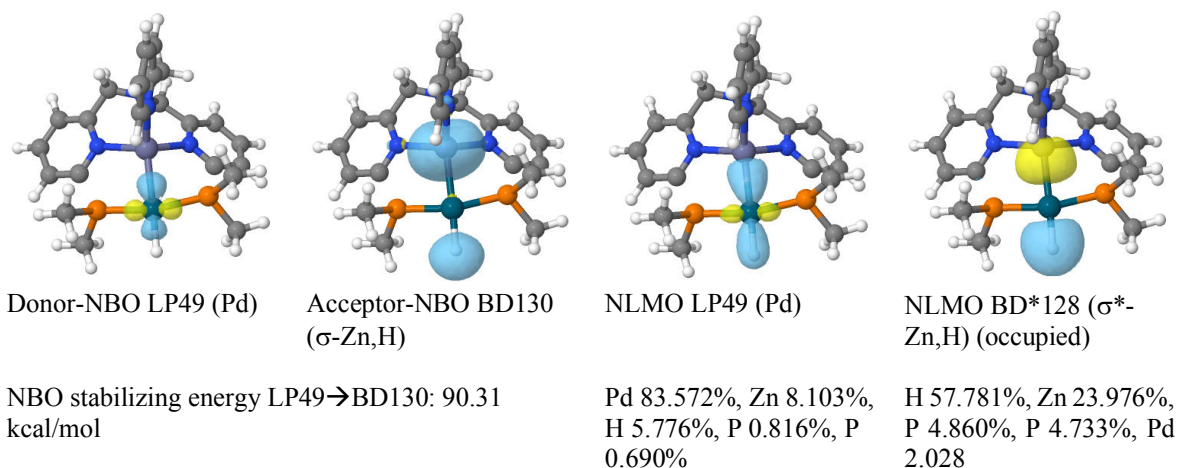


Fig. 12. NBO/NLMO analysis of **7-Zn**.

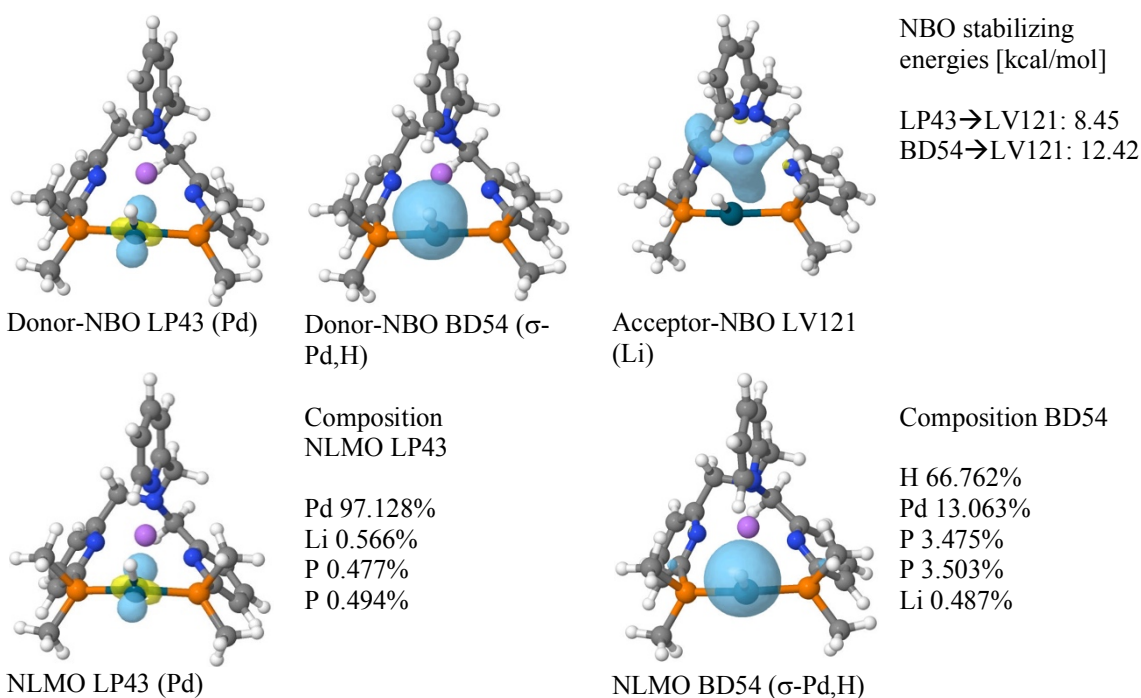


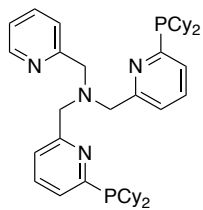
Fig. 13. NBO/NLMO analysis of **7-Li**.

Summary

Possible intermediates of CO₂ hydrosilylation were optimized by DFT calculations. These results suggest an intermediate Pd⁰-H hydride rather than a Pd^{II}-silylhydride formed by oxidative addition. This mechanism corresponds to the one suggest by Lu for her Ga/Ni catalyst system. It explains the beneficial effect of the CsOPiv additive. NBO/NLMO show a relevant stabilization of the Zn^{II} ligand of the Pd⁰-H, which is not observed for Li^I. This deviating stabilization could be responsible for the different catalytic activity.

5 Spectra

^1H NMR



DCPTPA

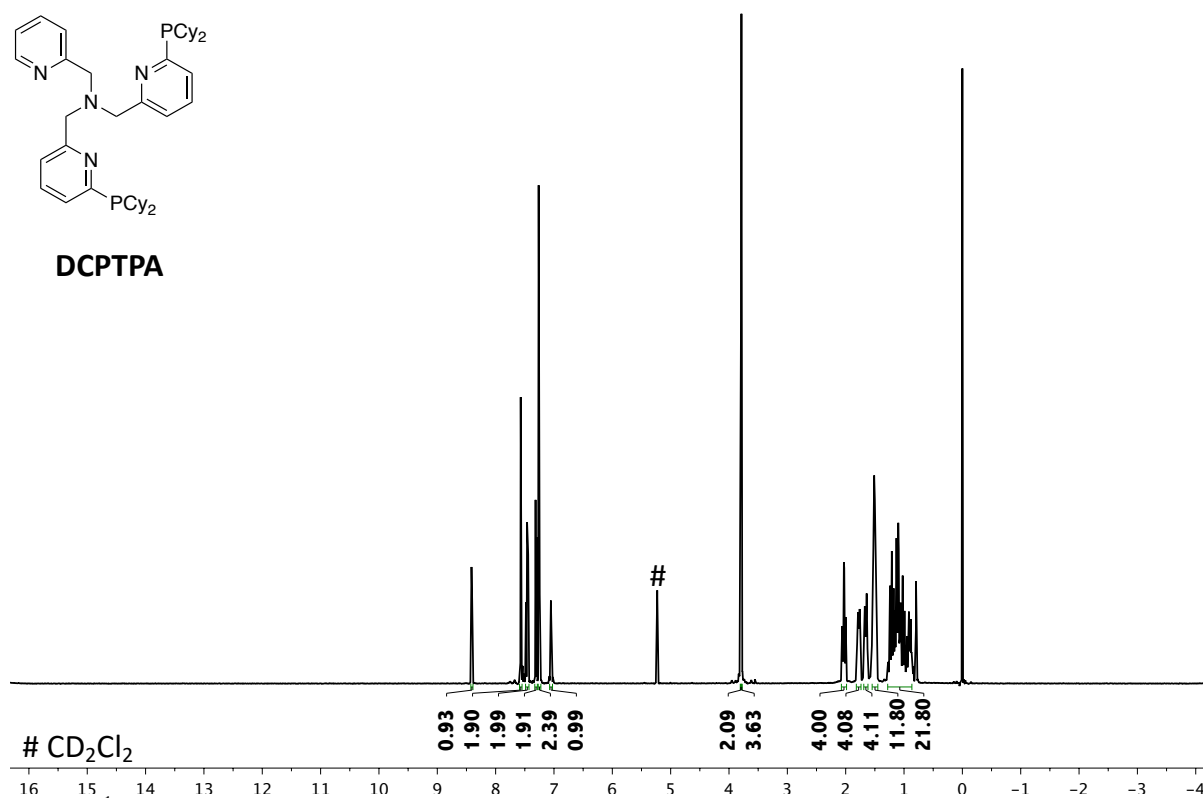
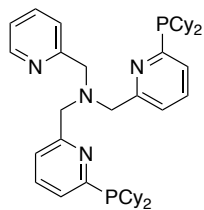


Fig. S14. ^1H NMR (400.3 MHz, DCM-d_2) of DCPTPA.

^{31}P NMR



DCPTPA

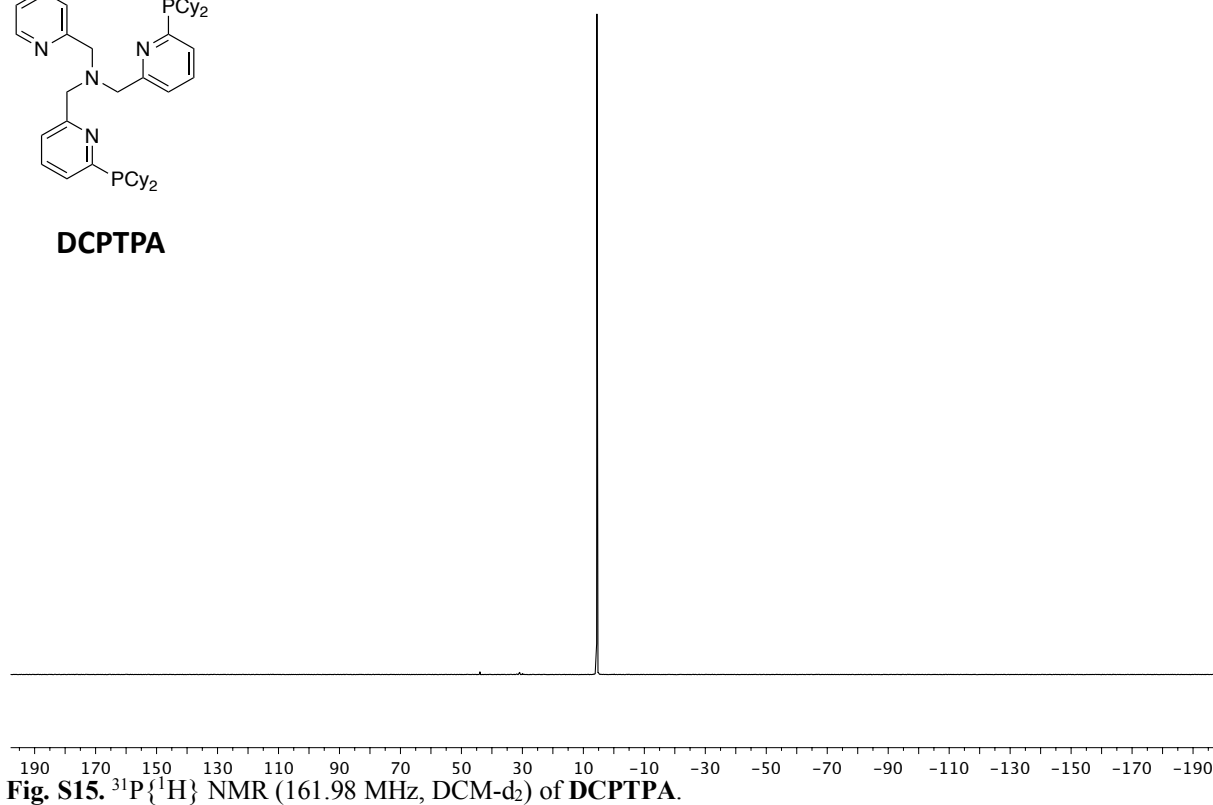
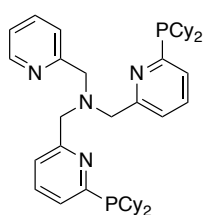


Fig. S15. $^{31}\text{P}\{^1\text{H}\}$ NMR (161.98 MHz, DCM-d_2) of DCPTPA.

^{13}C NMR



DCPTPA

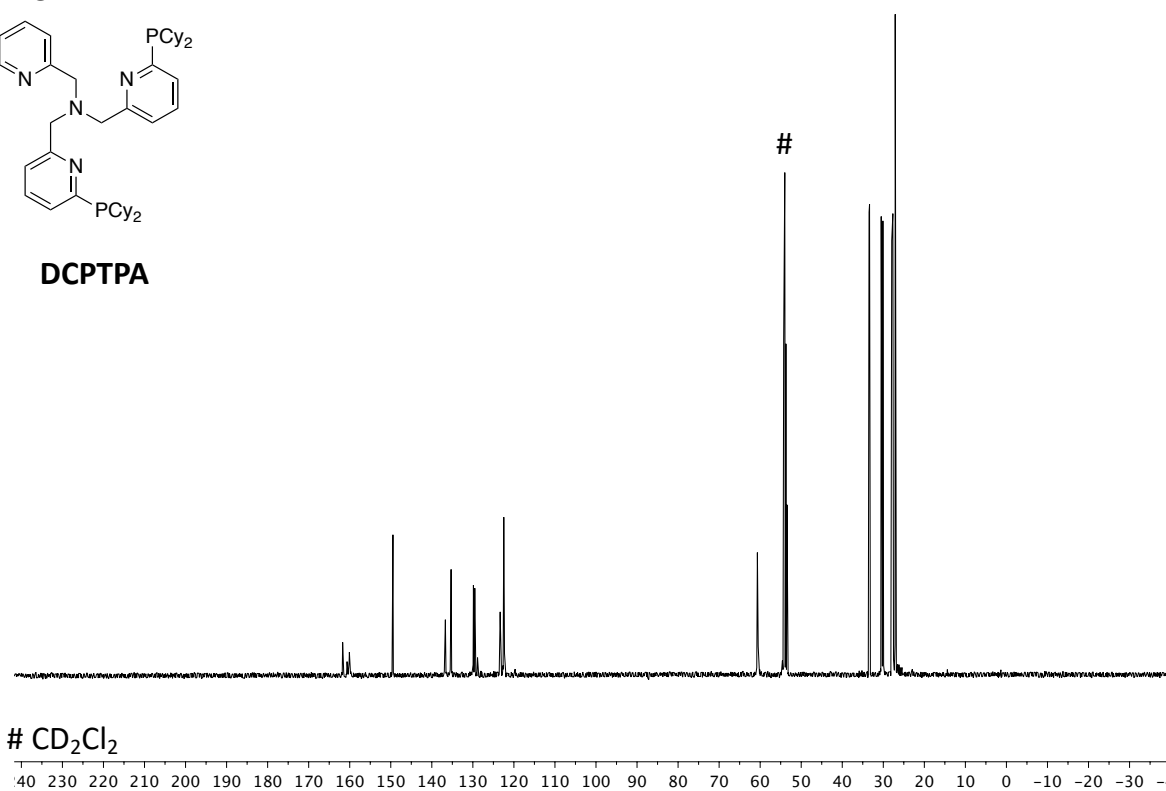


Fig. S16. $^{13}\text{C}\{^1\text{H}\}$ NMR (100.62 MHz, DCM-d_2) of DCPTPA.

^1H NMR

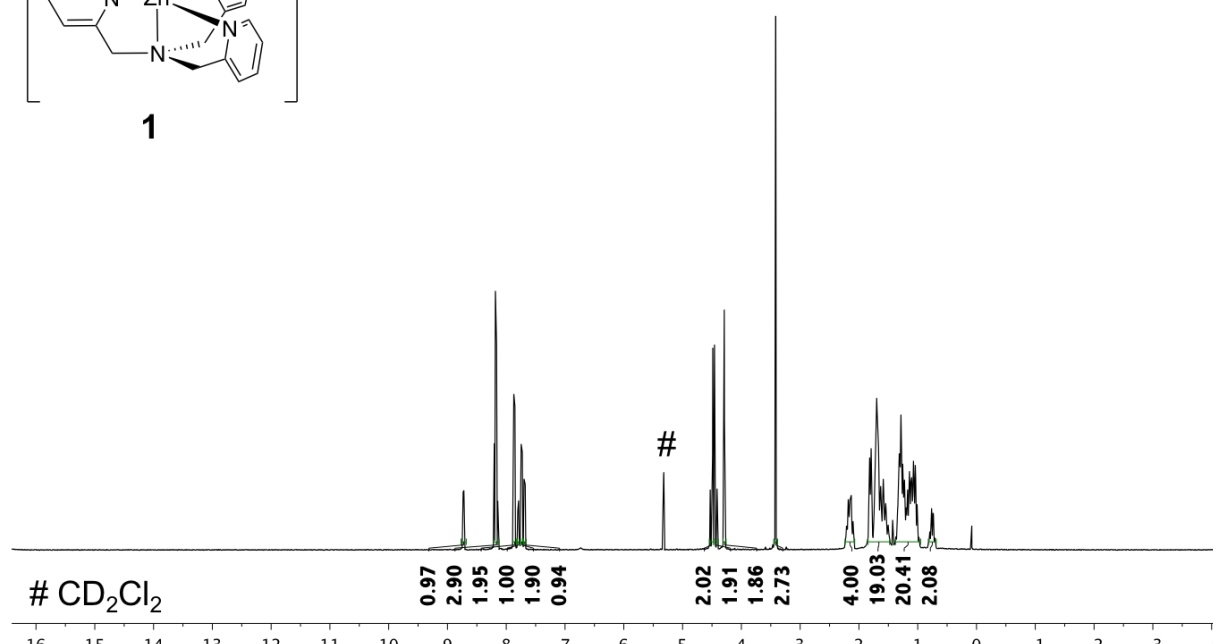
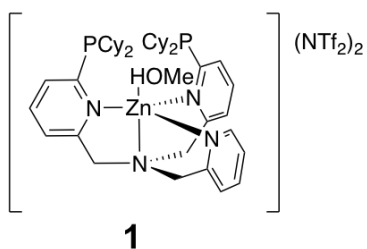


Fig. S17. ^1H NMR (400.3 MHz, DCM-d_2) of $[(\text{dcptpa})\text{Zn}](\text{NTf}_2)_2$.

³¹P NMR

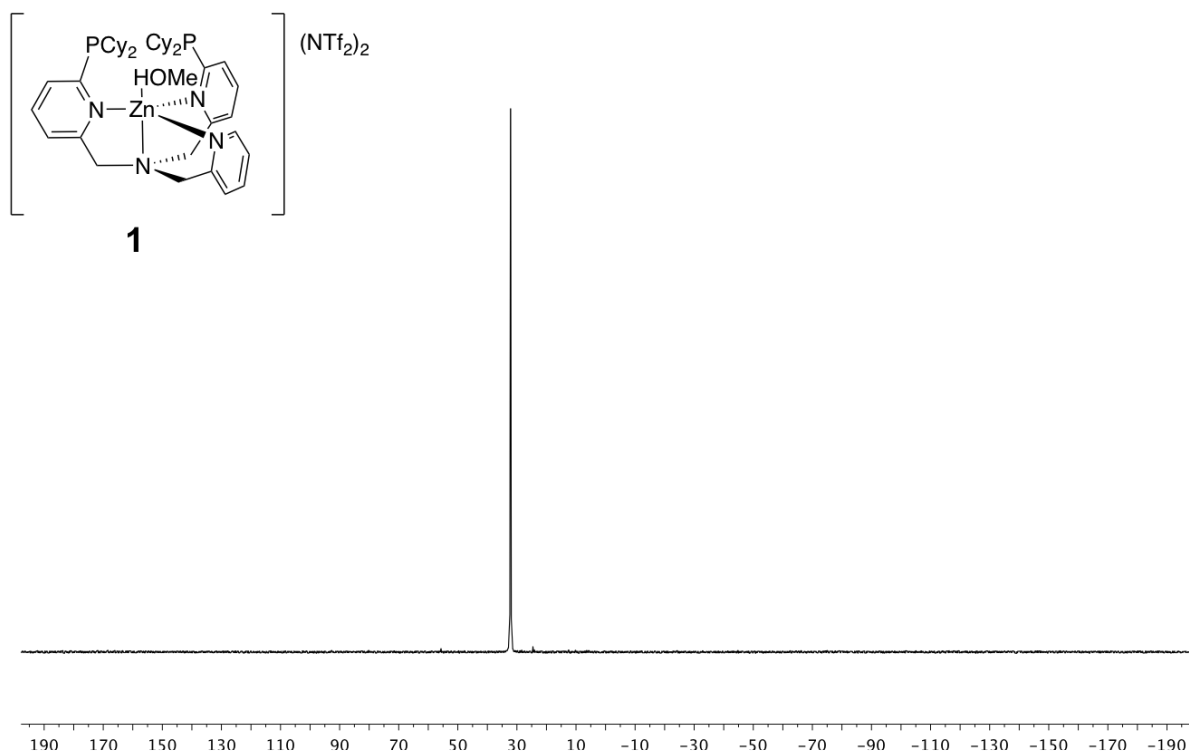


Fig. S18. ³¹P NMR (400.3 MHz, DCM-d₂) of $[(\text{deftpa})\text{Zn}](\text{NTf}_2)_2$.

¹³C NMR

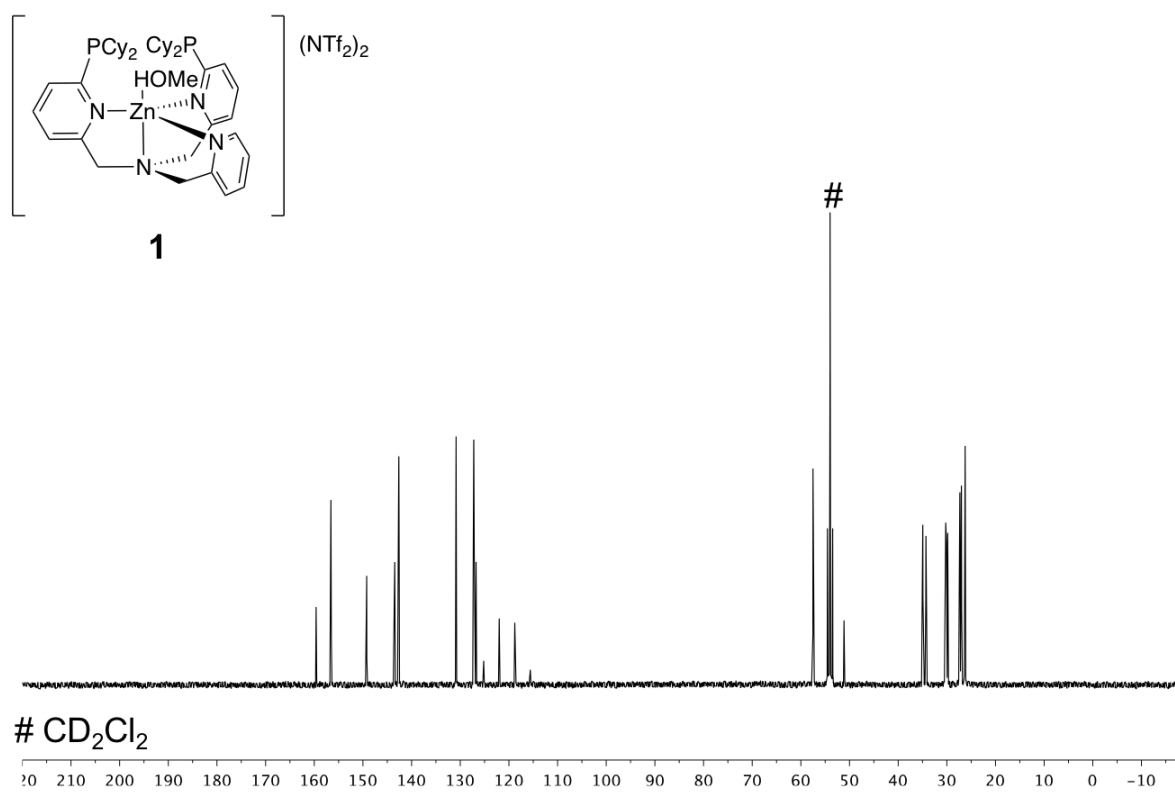


Fig. S19. ¹³C{¹H} NMR (100.62 MHz, DCM-d₂) of $[(\text{deftpa})\text{Zn}](\text{NTf}_2)_2$.

^1H NMR

$[(\text{dcptpa})\text{Pd}] \mathbf{2}$

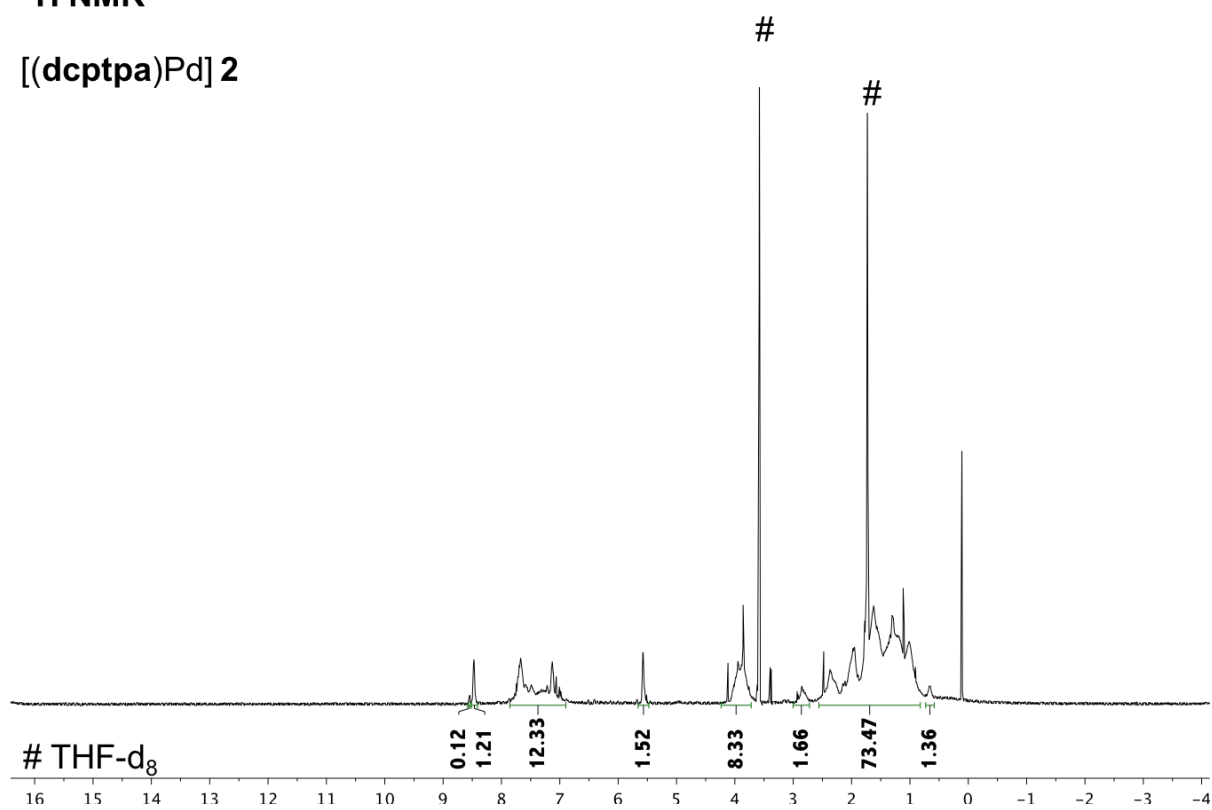


Fig. S20. ^1H NMR (400.3 MHz, THF- d_8) of **2**.

^{31}P NMR

$[(\text{dcptpa})\text{Pd}] \mathbf{2}$

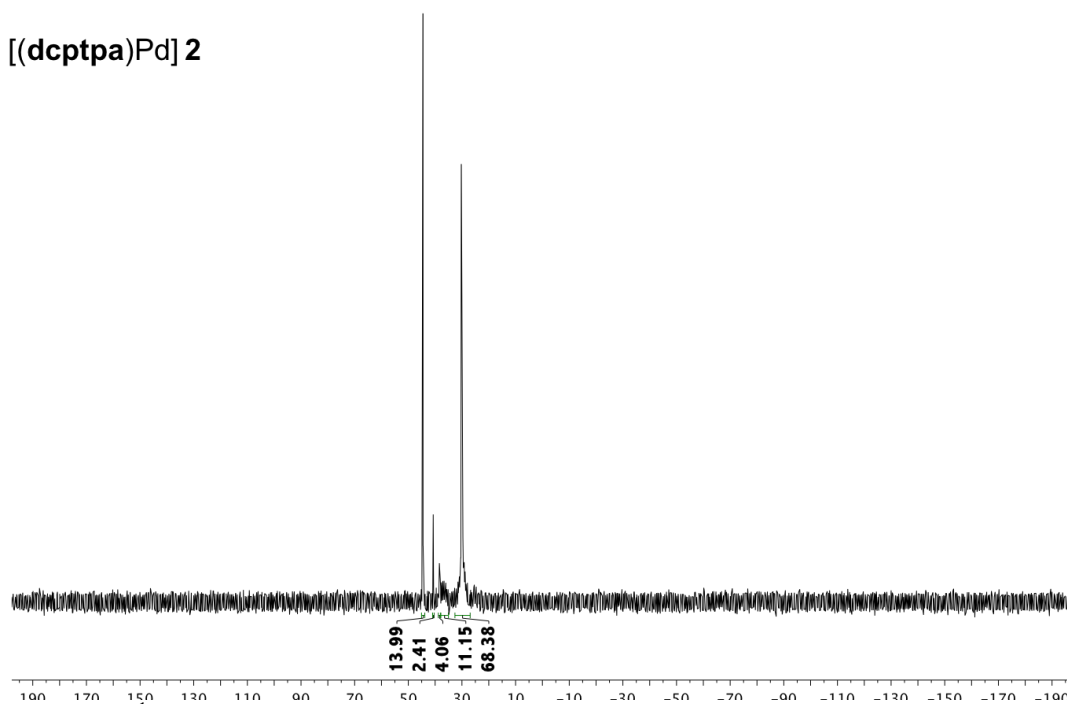


Fig. S21. $^{31}\text{P}\{^1\text{H}\}$ NMR (161.98 MHz, THF- d_8) of **2**.

¹H NMR

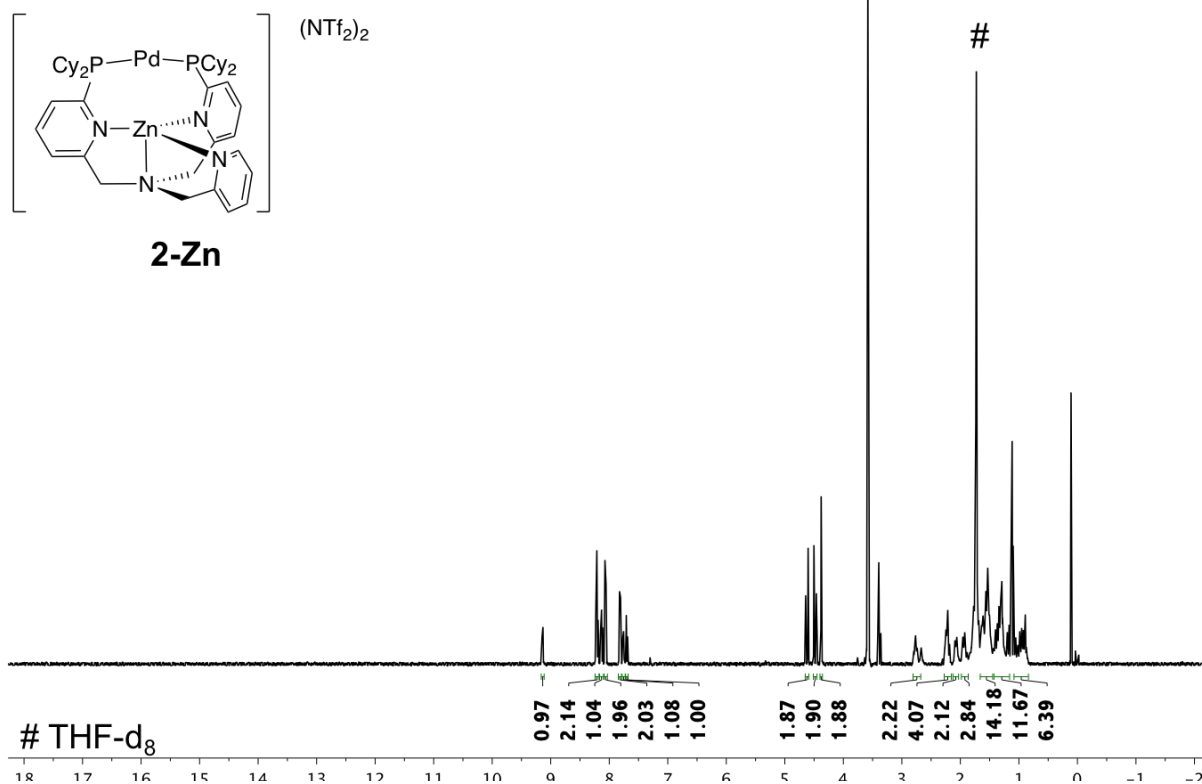


Fig. S22. ¹H NMR (400.3 MHz, THF-d₈) of **2-Zn**.

³¹P NMR

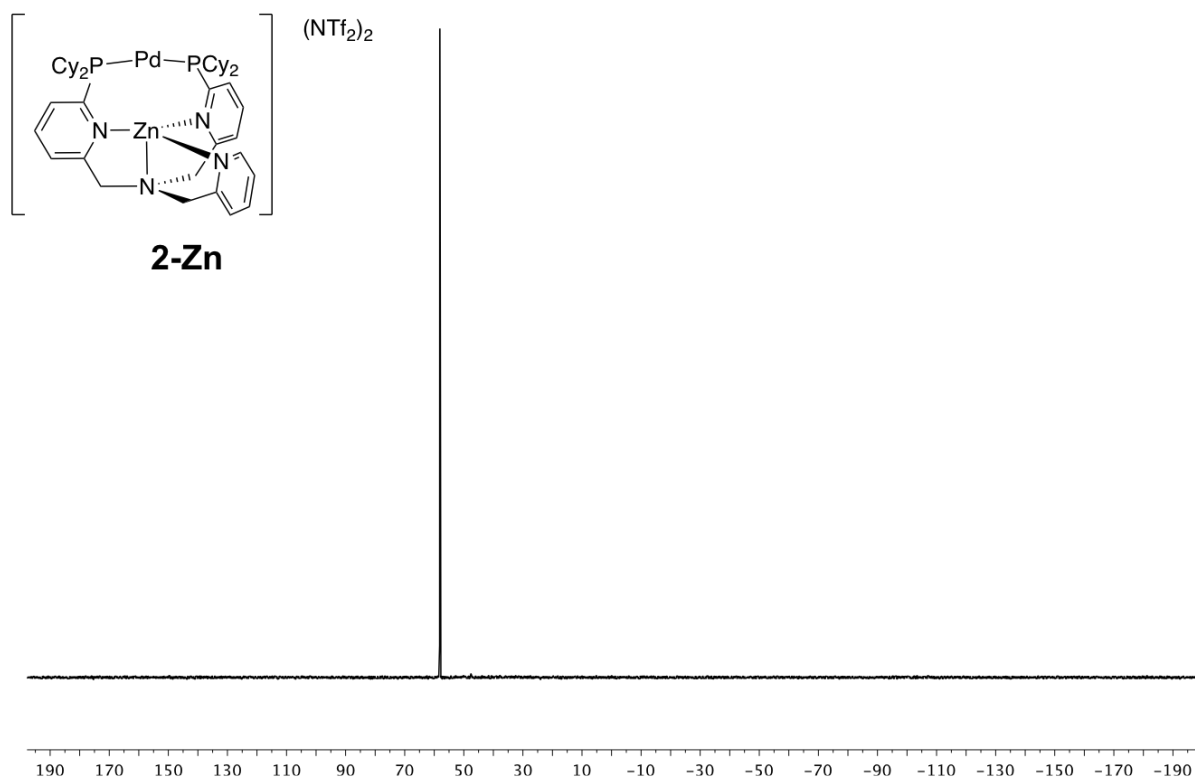


Fig. S23. ³¹P{¹H} NMR (161.98 MHz, THF-d₈) of **2-Zn**.

¹³C NMR

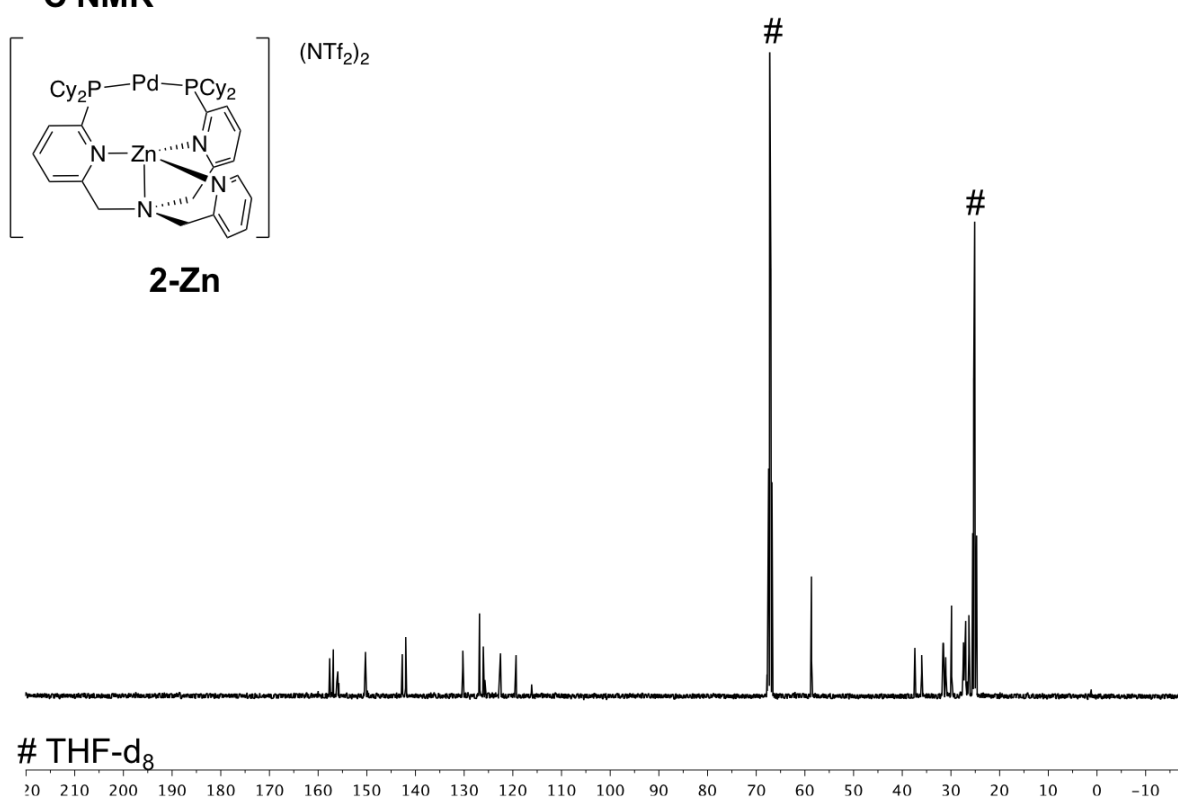


Fig. S24. ¹³C{¹H} NMR (100.67 MHz, THF-d₈) of **2-Zn**.

¹⁹F NMR

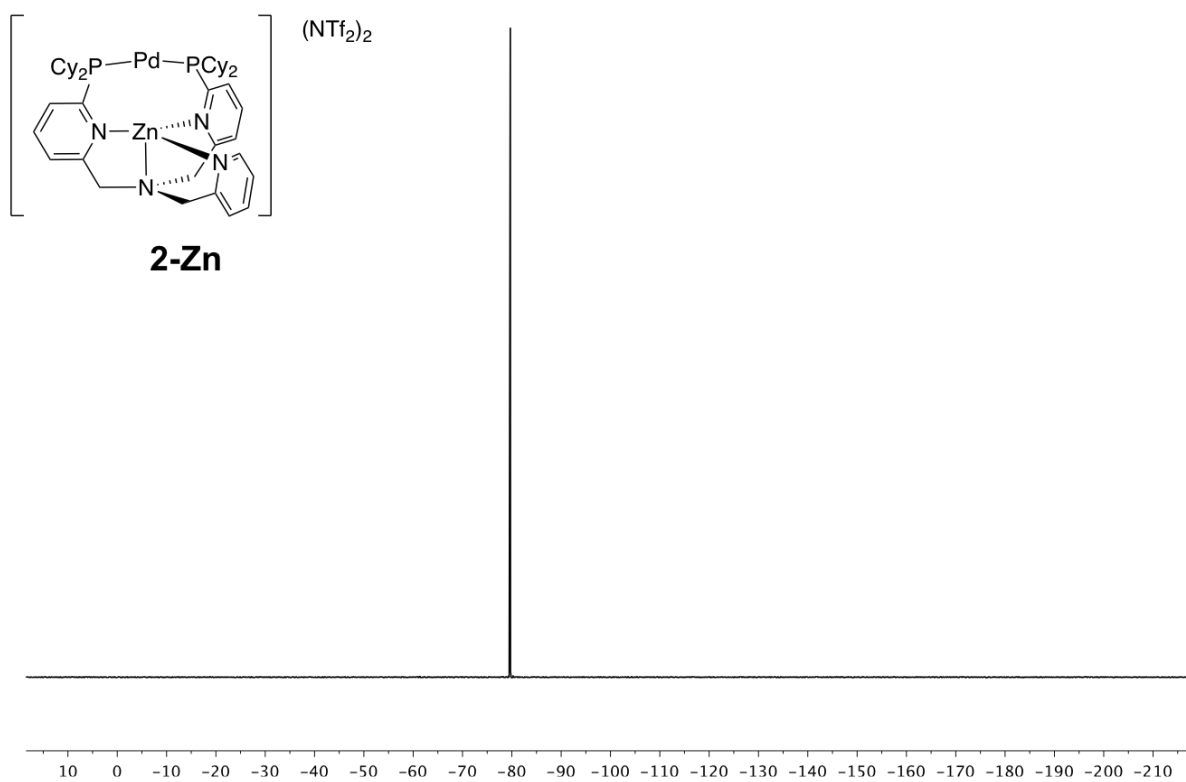


Fig. S25. ¹⁹F{¹H} NMR (376.62 MHz, THF-d₈) of **2-Zn**.

¹H NMR

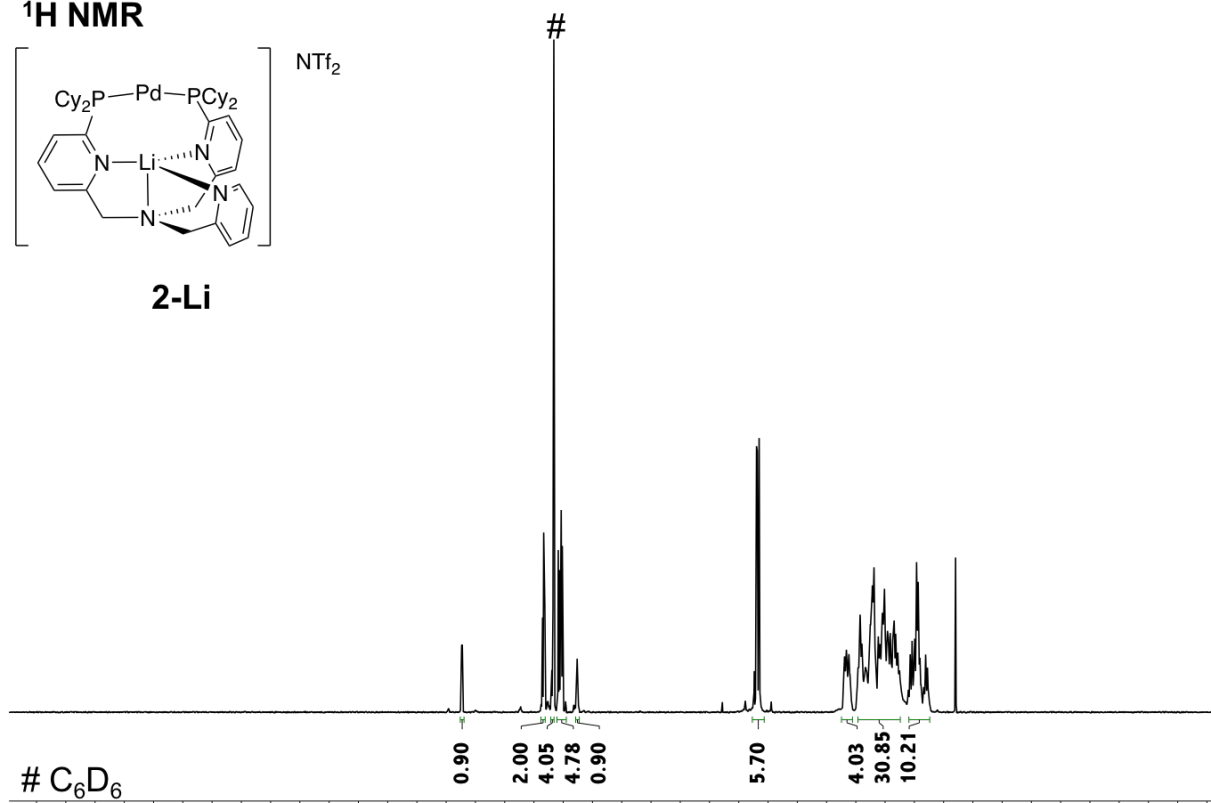
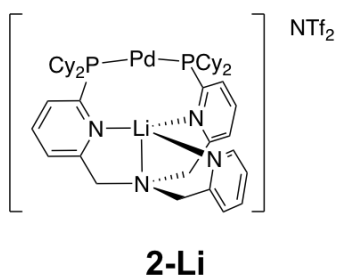


Fig. S26. ¹H NMR (400.3 MHz, C₆D₆) of **2-Li**.

³¹P NMR

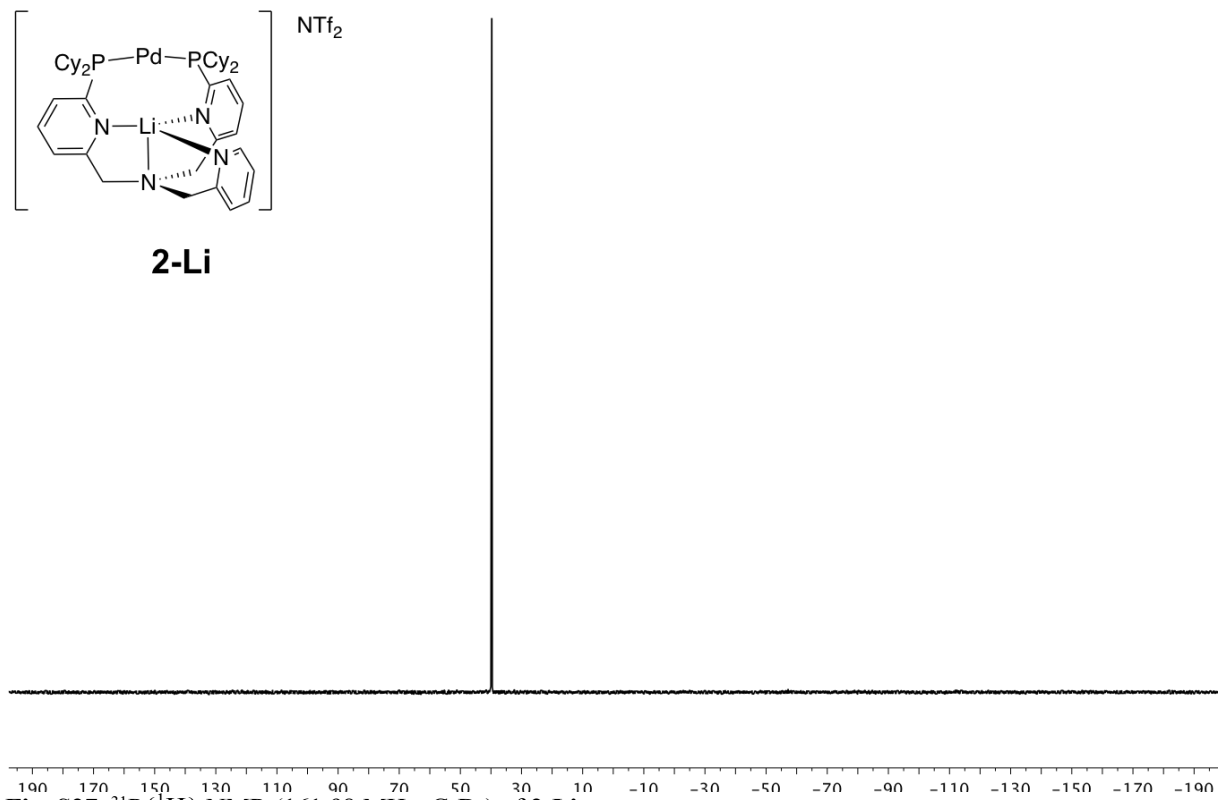
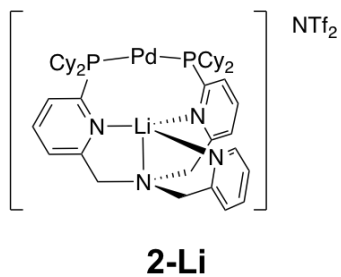
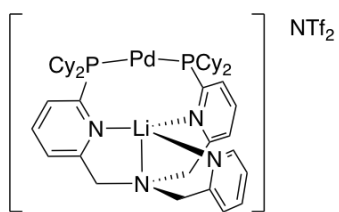
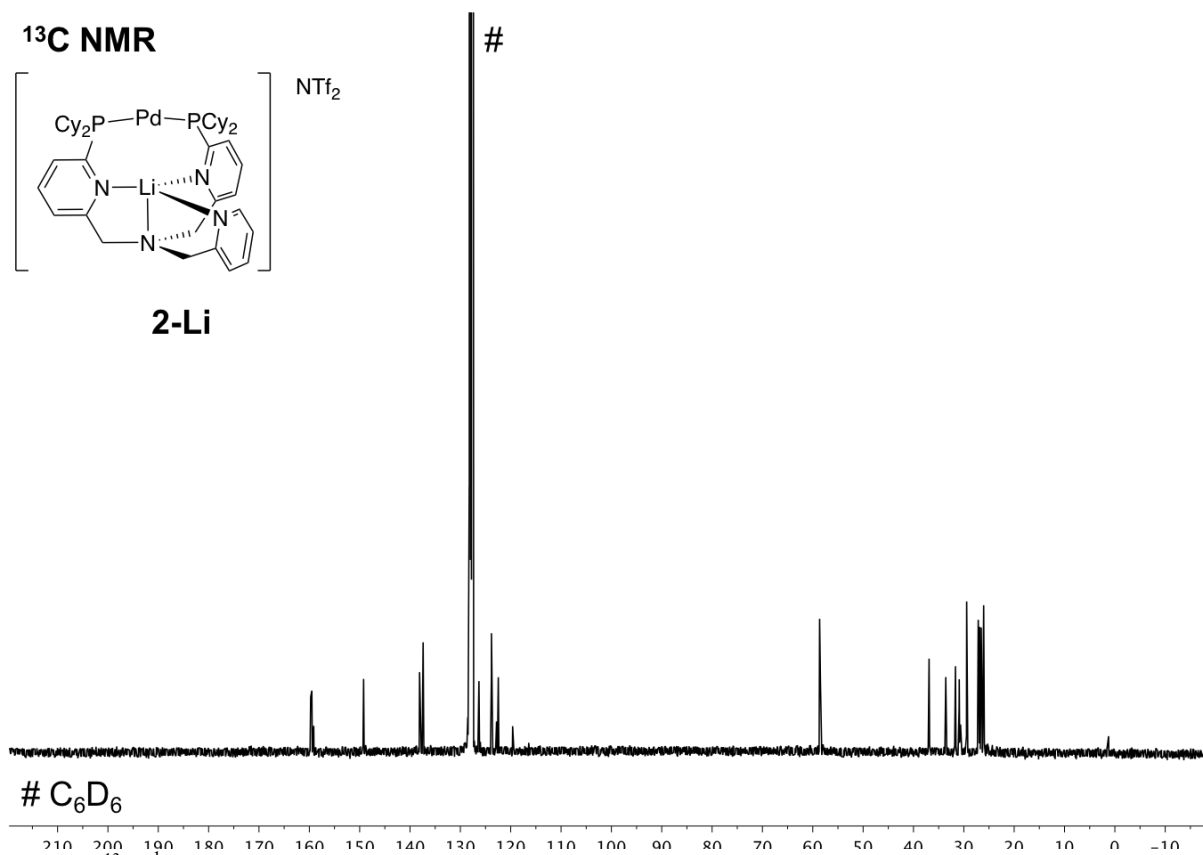
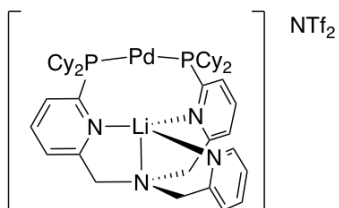
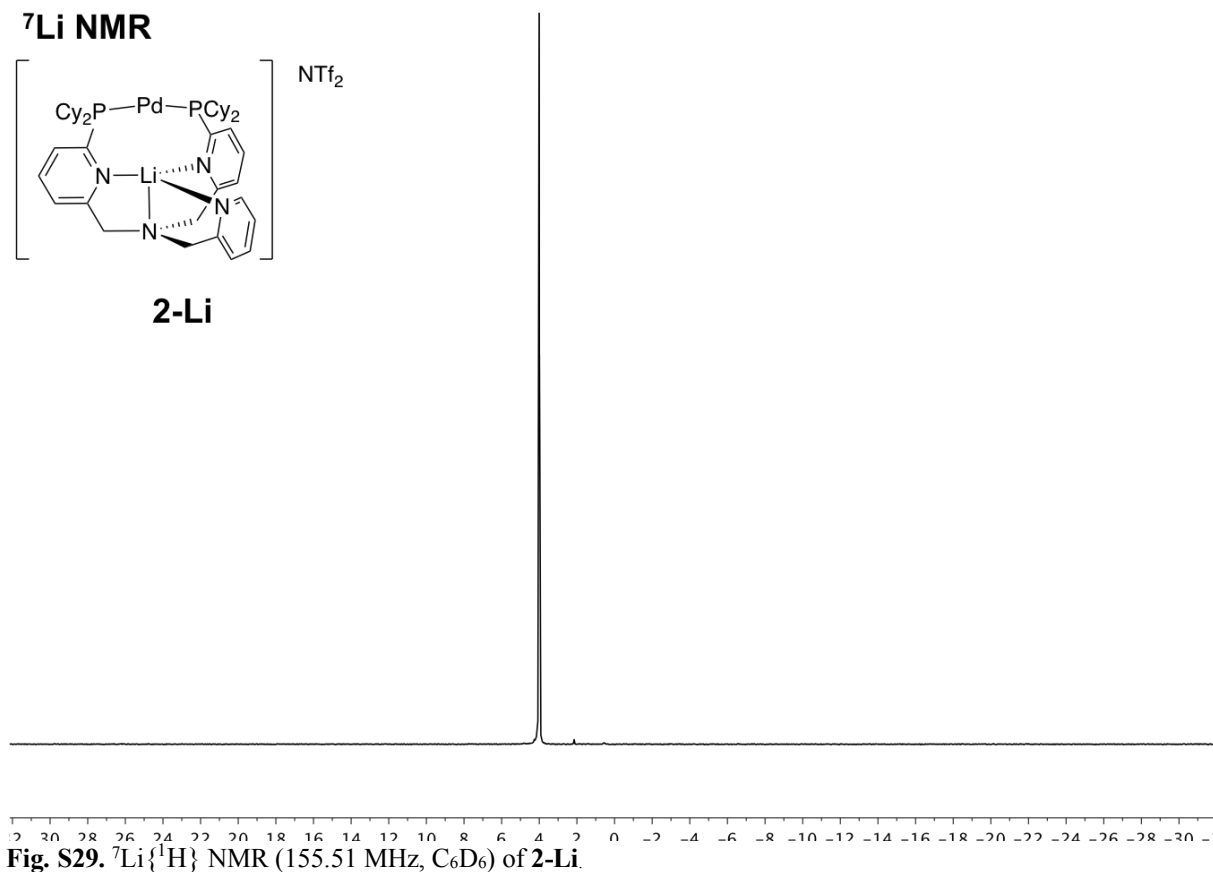


Fig. S27. ³¹P{¹H} NMR (161.98 MHz, C₆D₆) of **2-Li**.

¹³C NMR**2-Li****Fig. S28.** ¹³C{¹H} NMR (100.67 MHz, C₆D₆) of **2-Li**.**⁷Li NMR****2-Li****Fig. S29.** ⁷Li{¹H} NMR (155.51 MHz, C₆D₆) of **2-Li**.

¹⁹F NMR

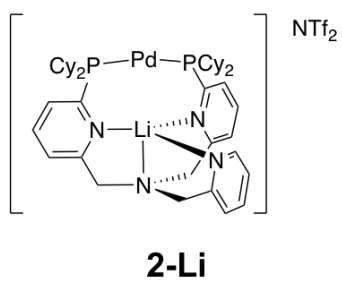


Fig. S30. ¹⁹F{¹H} NMR (376.62 MHz, C₆D₆) of **2-Li**.

¹H NMR

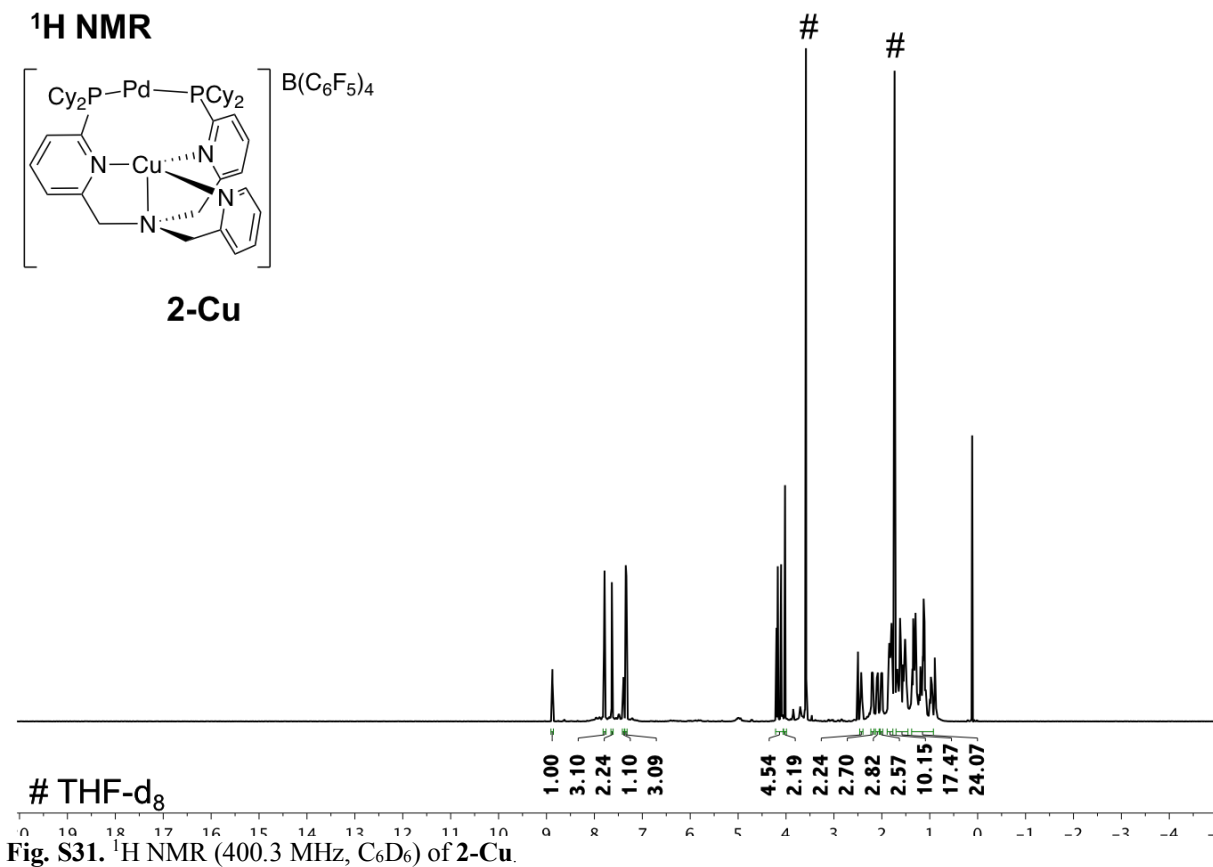
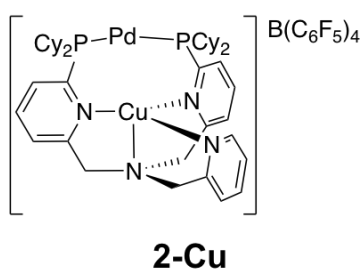


Fig. S31. ¹H NMR (400.3 MHz, C₆D₆) of **2-Cu**.

³¹P NMR

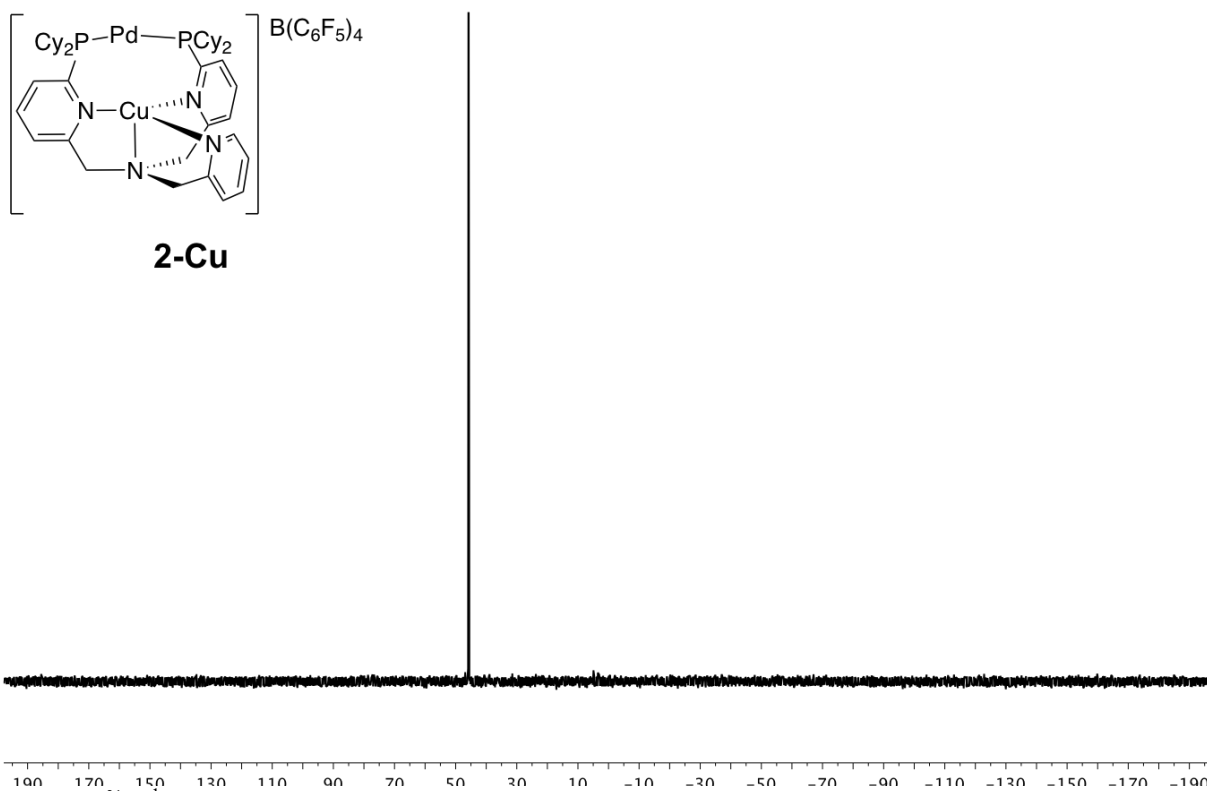


Fig. S32. $^{31}P\{^1H\}$ NMR (161.98 MHz, C_6D_6) of **2-Cu**.

¹³C NMR

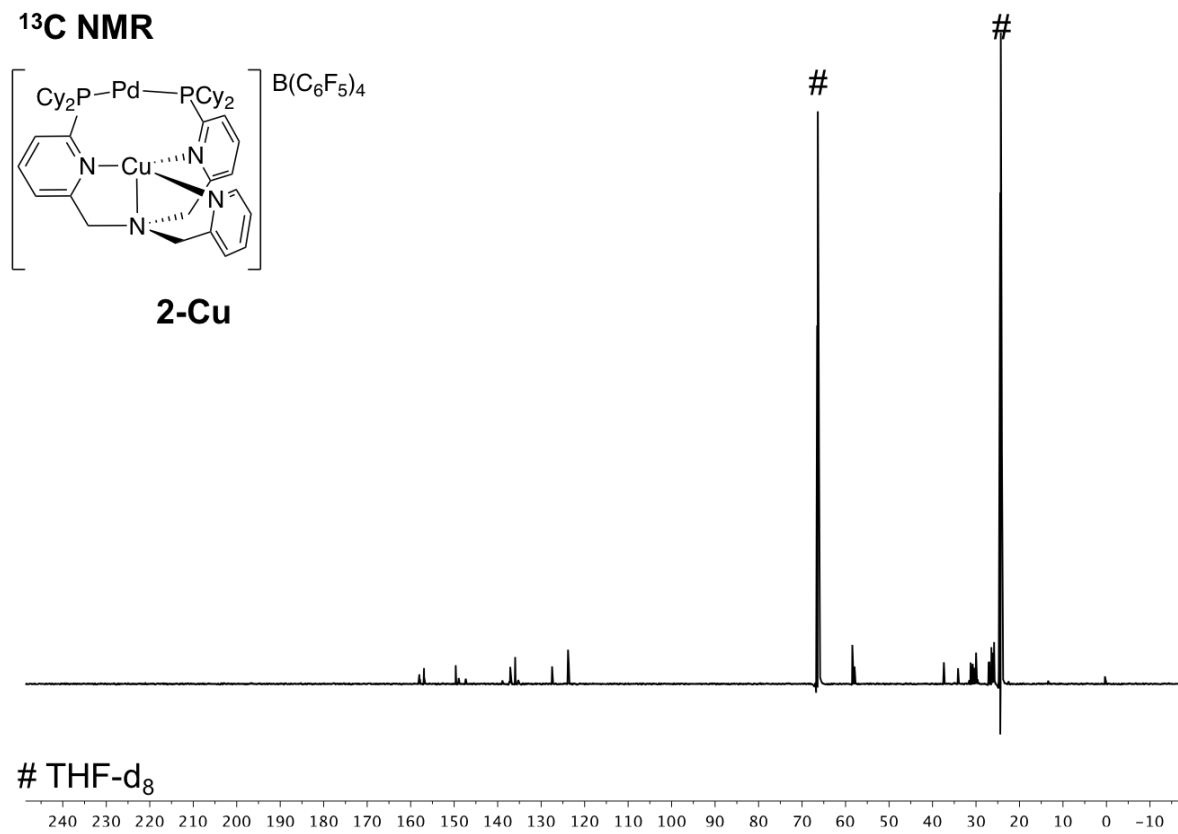


Fig. S33. $^{13}C\{^1H\}$ NMR (150.85 MHz, C_6D_6) of **2-Cu**.

^{11}B NMR

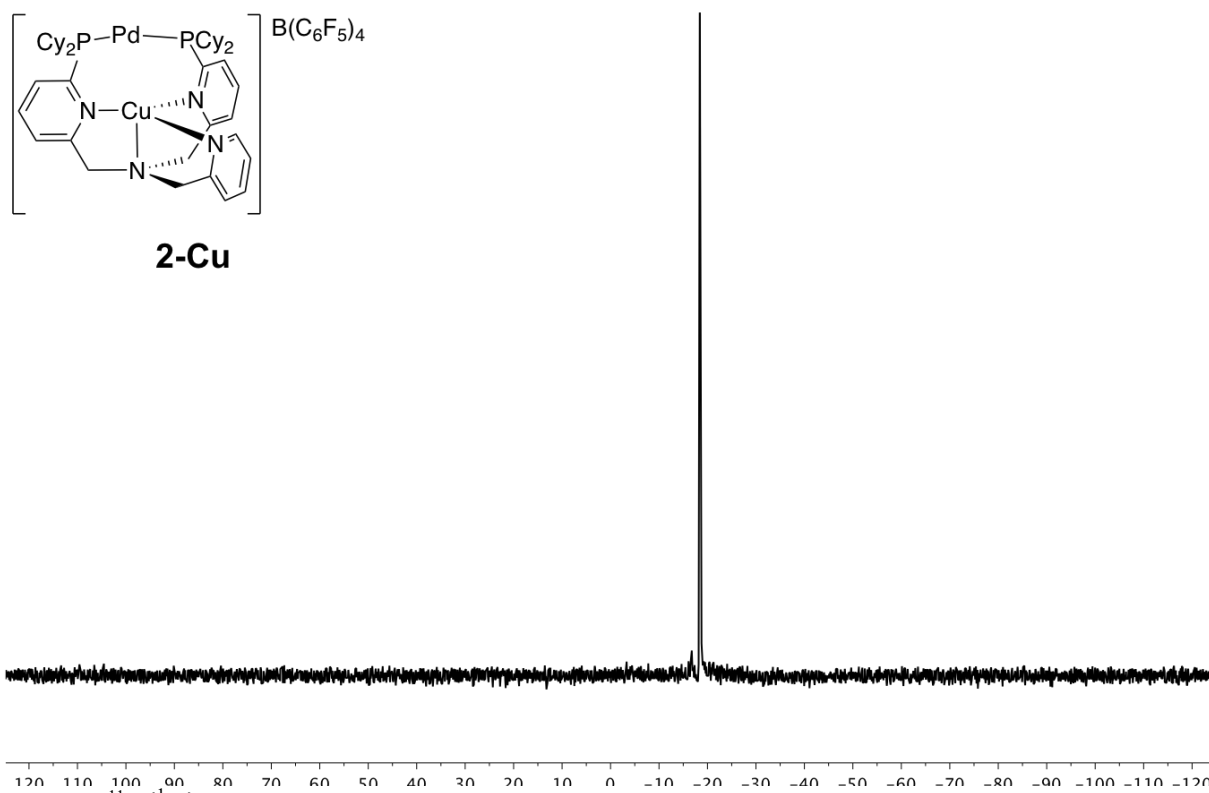


Fig. S34. $^{11}\text{B}\{^1\text{H}\}$ NMR (155.51 MHz, C_6D_6) of **2-Cu**.

^{19}F NMR

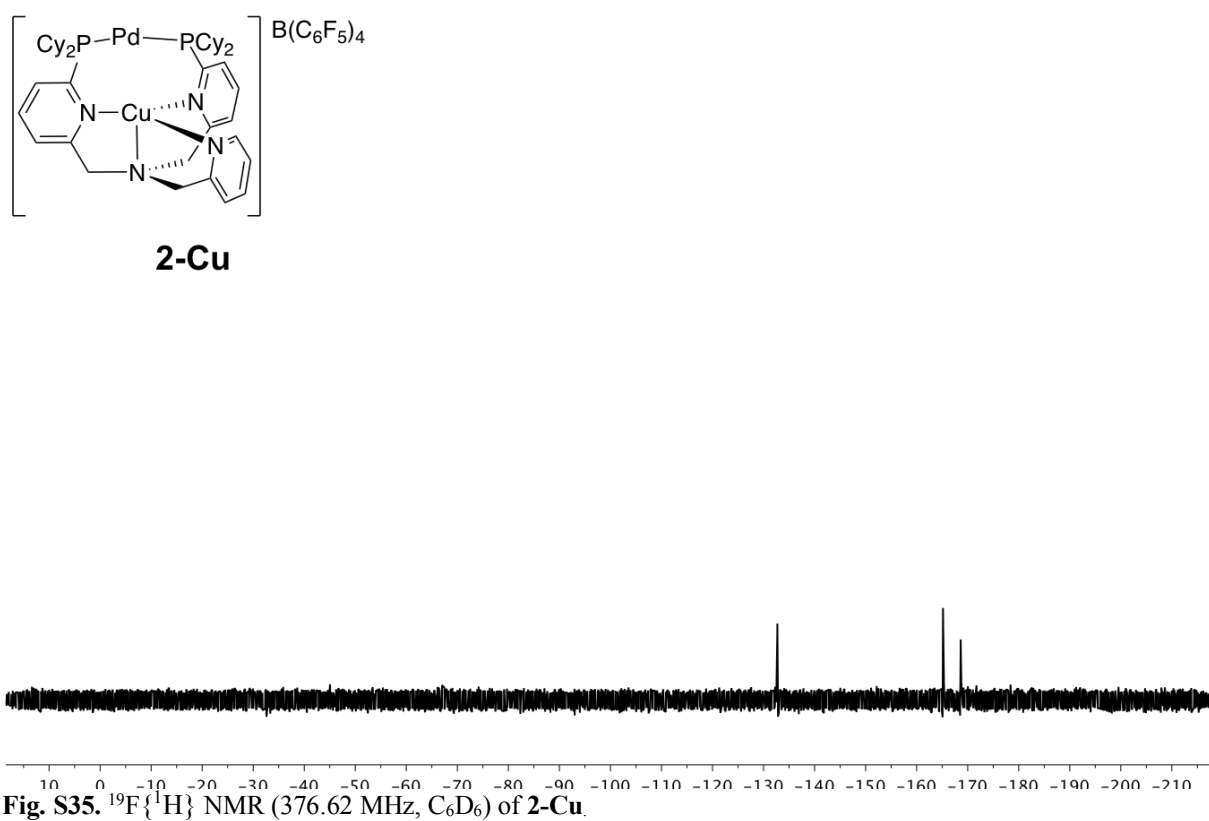
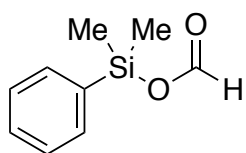


Fig. S35. $^{19}\text{F}\{^1\text{H}\}$ NMR (376.62 MHz, C_6D_6) of **2-Cu**.

¹H NMR



HCO(O)SiMe₂Ph

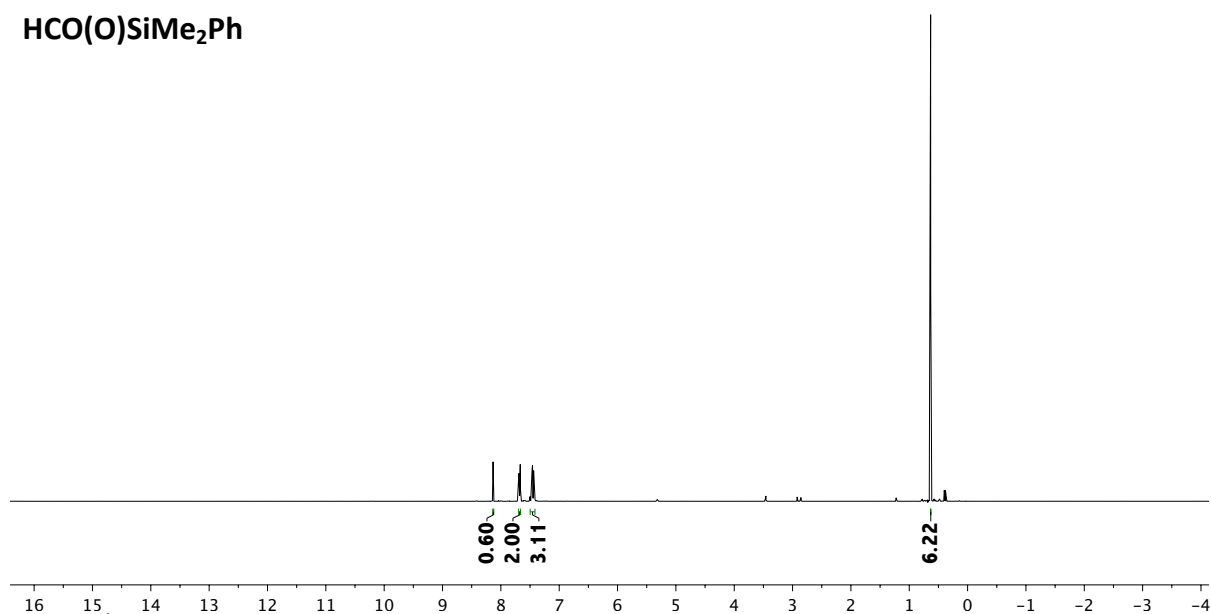
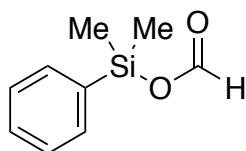


Fig. S36. ¹H NMR (400.3 MHz, C₆D₆) of HCO(O)SiMe₂Ph.

¹³C NMR



HCO(O)SiMe₂Ph

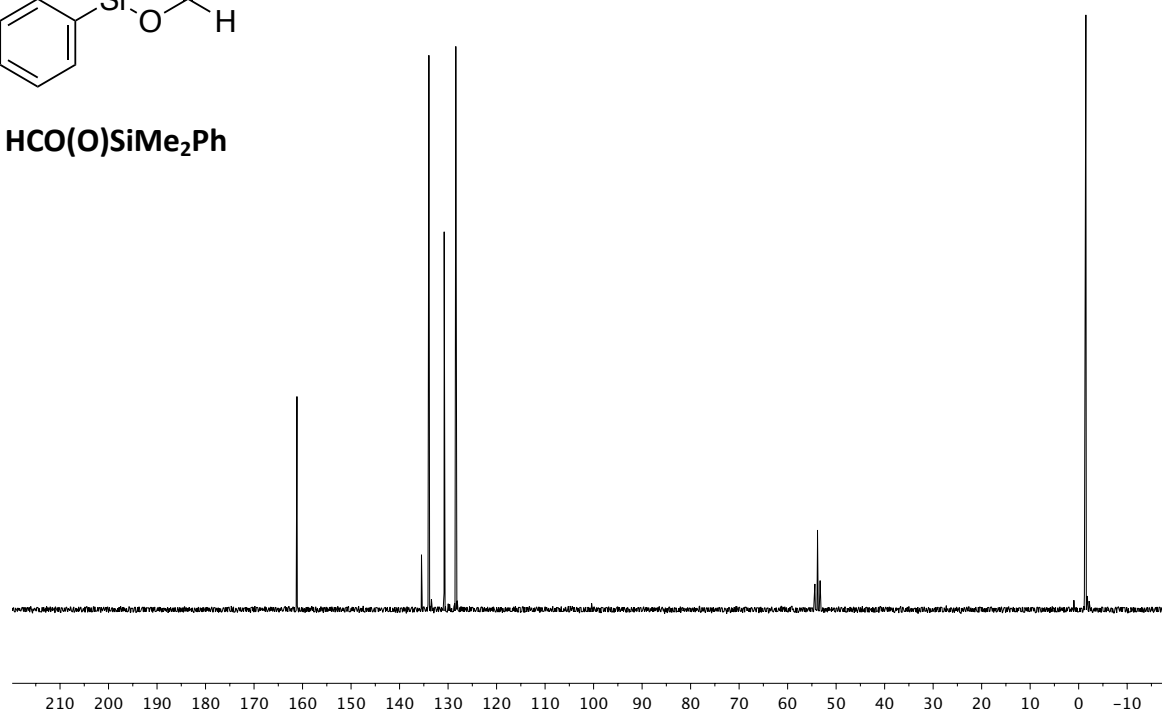
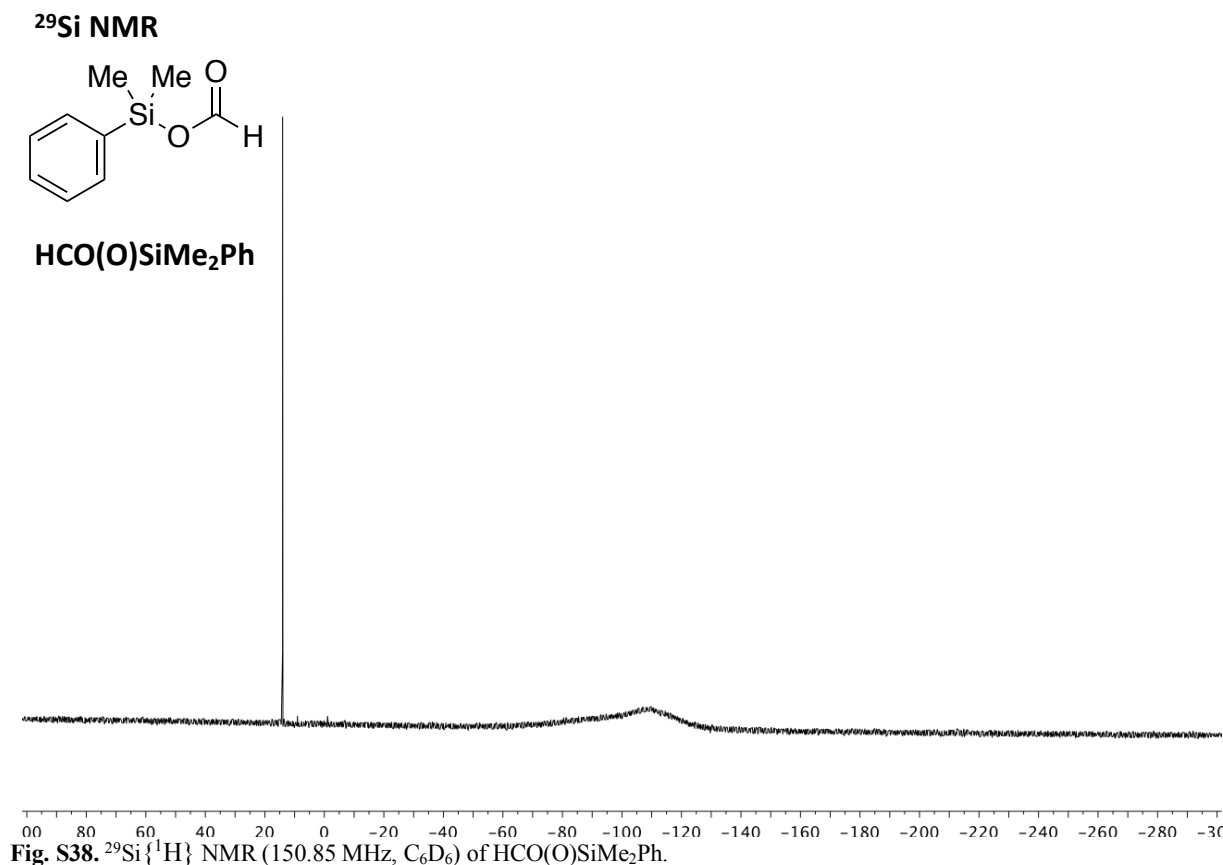


Fig. S37. ¹³C{¹H} NMR (150.85 MHz, C₆D₆) of HCO(O)SiMe₂Ph.



6 References

1. G. R. Fulmer, A. J. M. Miller, N. H. Sherden, H. E. Gottlieb, A. Nudelman, B. M. Stoltz, J. E. Bercaw and K. I. Goldberg, *Organometallics*, 2010, **29**, 2176-2179.
2. K. Issleib and A. Brack, *Z. Anorg. Allg. Chem.*, 1954, **277**, 259 - 270.
3. E. C. Ashby, R. N. DePriest and W.-Y. Su, *Organometallics*, 1984, **3**, 1718 - 1727.
4. Y. Zhang, Z. Yuan and R. J. Puddephatt, *Chem. Mater.*, 1998, **10**, 2293-2300.
5. Y. Tatsuno, T. Yoshida and M. Seiotsuka, *Inorg. Synth*, 1979, **19**, 220-223.
6. R. G. Hicks, B. D. Koivisto and M. T. Lemaire, *Org. Lett.*, 2004, **6**, 1887 - 1890.
7. D. Schnieders, M. Merkel, S. M. Baldeau and B. Krebs, *Eur. J. Inorg. Chem.*, 2004, **2004**, 783 - 790.
8. D. Schnieders, M. Merkel, S. M. Baldeau and B. Krebs, *Z. Anorg. Allg. Chem.*, 2004, **630**, 1210-1214.
9. A. Jansen and S. Pitter, *J. Mol. Catal. A: Chem.*, 2004, **217** 41-45.
10. J. Takaya and N. Iwasawa, *J. Am. Chem. Soc.*, 2017, **139**, 6074-6077.
11. K. Motokura, D. Kashiwame, N. Takahashi, A. Miyaji and T. Baba, *Chem. Eur. J.*, 2013, **19**, 10030-10037.
12. L. Zhang, J. Cheng and Z. Hou, *Chem. Commun.*, 2013, **49**, 4782-4784.
13. P. Ríos, J. Díez, J. López-Serrano, A. Rodríguez and S. Conejero, *Chem. Eur. J.*, 2016, **22**, 16791-16795.
14. A. Jansen, H. Görls and S. Pitter, *Organometallics*, 2000, **19**, 135-138.

15. M. L. Scheuermann, S. P. Semproni, I. Pappas and P. J. Chirik, *Inorg. Chem.*, 2014, **53**, 9463-9465.
16. S. Itagaki, K. Yamaguchi and N. Mizuno, *J. Mol. Catal. A: Chem.*, 2013, **366**, 347-352.
17. R. Lalrempuia, M. Iglesias, V. Polo, P. J. Sanz Miguel, F. J. Fernández-Alvarez, J. J. Pérez-Torrente and L. A. Oro, *Angew. Chem. Int. Ed.*, 2012, **51**, 12824-12827.
18. G. Süss-Fink and J. Reiner, *J. Organomet. Chem.*, 1981, **221**, C36 - C38.
19. W. Sattler and G. Parkin, *J. Am. Chem. Soc.*, 2012, **134**, 17462-17465.
20. SMART, *Bruker ACX Inc.*, 2001, Madison, Wisconsin, USA.
21. SAINT+, *Bruker AXS Inc.*, 2009, Madison, Wisconsin, USA.
22. SADABS, *Bruker ACX Inc.*, 2008, Madison, Wisconsin, USA.
23. O. V. Dolomanov, L. J. Bourhis, R. J. Gildea, J. A. K. Howard and H. Puschmann, *J. Appl. Cryst.*, 2009, **42**, 339-341.
24. G. M. Sheldrick, *Acta Cryst.*, 2008, **A64**, 112-122.
25. L. J. Bourhis, O. V. Dolomanov, R. J. Gildea, J. A. K. Howard and H. Puschmann, *Acta Cryst.*, 2015, **A71**, 59-75.
26. A. Spek, *Acta Cryst.*, 2015, **C71**, 9-18.
27. A. Spek, *J. Appl. Cryst.*, 2003, **36**, 7-13.
28. A. Spek, *Acta Cryst.*, 2009, **D65**, 148-155.
29. C. F. Macrae, I. J. Bruno, J. A. Chisholm, P. R. Edgington, P. McCabe, E. Pidcock, L. Rodriguez-Monge, R. Taylor, J. van de Streek and P. A. Wood, *J. Appl. Cryst.*, 2008, **41**, 466-470.
30. H.-O. Fröhlich, R. Wyrwa and H. Görls, *J. Organomet. Chem.*, 1993, **456**, 7-12.
31. M. D. Fryzuk, B. R. Lloyd, G. K. B. Clentsmith and S. J. Rettig, *J. Am. Chem. Soc.*, 1991, **113**, 4332-4334.
32. M. D. Fryzuk, B. R. Lloyd, G. K. B. Clentsmith and S. J. Rettig, *J. Am. Chem. Soc.*, 1994, **116**, 3804-3812.
33. R. J. Oeschger and P. Chen, *J. Am. Chem. Soc.*, 2017, **139**, 1069-1072.
34. I. P.-C. Liu, C.-H. Chen, C.-F. Chen, G.-H. Lee and S.-M. Peng, *Chem. Commun.*, 2009, DOI: 10.1039/B817032K, 577-579.
35. M. Tanabe, N. Ishikawa, M. Chiba, T. Ide, K. Osakada and T. Tanase, *J. Am. Chem. Soc.*, 2011, **133**, 18598-18601.
36. I. P.-C. Liu, G.-H. Lee, S.-M. Peng, M. Bénard and M.-M. Rohmer, *Inorg. Chem.*, 2007, **46**, 9602-9608.
37. O. Crespo, M. C. Gimeno, A. Laguna, O. Lehtonen, I. Ospino, P. Pyykkö and M. D. Villacampa, *Chem. Eur. J.*, 2014, **20**, 3120-3127.
38. N. Ichieda, T. Kamimura, Y. Wasada-Tsutsui, Y. Funahashi, T. Ozawa, K. Jitsukawa and H. Masuda, *Chem. Lett.*, 2008, **37**, 1220-1221.
39. B. Wu, W.-J. Zhang, S.-Y. Yu, T.-L. Sheng and X.-T. Wu, *J. Organomet. Chem.*, 1997, **545-546**, 587-589.
40. M. Tanabe, R. Yumoto, T. Yamada, T. Fukuta, T. Hoshino, K. Osakada and T. Tanase, *Chem. Eur. J.*, 2016, **23**, 1386-1392.
41. T. Nakajima, H. Konomoto, H. Ogawa and Y. Wakatsuki, *J. Organomet. Chem.*, 2007, **692**, 5071-5080.

42. M. Ebihara, K. Tokoro, M. Maeda, M. Ogami, K. Imaeda, K. Sakurai, H. Masuda and T. Kawamura, *J. Chem. Soc. Dalton Trans.*, 1994, DOI: 10.1039/DT9940003621, 3621-3635.
43. K. Freitag, M. Molon, P. Jerabek, K. Dilchert, C. Rösler, R. W. Seidel, C. Gemel, G. Frenking and R. A. Fischer, *Chem. Sci.*, 2016, **7**, 6413-6421.
44. R. J. Oeschger and P. Chen, *Organometallics*, 2017, **36**, 1465-1468.
45. T. Cadenbach, T. Bollermann, C. Gemel, M. Tombul, I. Fernandez, M. V. Hopffgarten, G. Frenking and R. A. Fischer, *J. Am. Chem. Soc.*, 2009, **131**, 16063-16077.
46. T. Bollermann, K. Freitag, C. Gemel, R. W. Seidel, M. von Hopffgarten, G. Frenking and R. A. Fischer, *Angew. Chem. Int. Ed.*, 2010, **50**, 772-776.
47. T. Bollermann, K. Freitag, C. Gemel, M. Molon, R. W. Seidel, M. von Hopffgarten, P. Jerabek, G. Frenking and R. A. Fischer, *Inorg. Chem.*, 2011, **50**, 10486-10492.
48. T. Bollermann, T. Cadenbach, C. Gemel, M. von Hopffgarten, G. Frenking and R. A. Fischer, *Chem. Eur. J.*, 2010, **16**, 13372-13384.
49. T. Bollermann, K. Freitag, C. Gemel, R. W. Seidel and R. A. Fischer, *Organometallics*, 2011, **30**, 4123-4127.
50. M. Molon, C. Gemel and R. A. Fischer, *Dalton Trans.*, 2014, **43**, 3114-3120.
51. C. M. Fafard, C.-H. Chen, B. M. Foxman and O. V. Ozerov, *Chem. Commun.*, 2007, **43**, 4465-4467.
52. F. Furche, R. Ahlrichs, C. Hattig, W. Klopper, M. Sierka and F. Weigend, *WIREs Comput. Mol. Sci.*, 2014, **4**, 91-100.
53. F. Weigend, *Phys. Chem. Chem. Phys.*, 2006, **8**, 1057-1065.
54. S. Grimme, J. Antony, S. Ehrlich and H. Krieg, *J. Chem. Phys.*, 2010, **132**, 154104-154123.
55. J. P. Perdew, *Phys. Rev. B*, 1986, **33**, 8822-8824.
56. F. Weigend and R. Ahlrichs, *Phys. Chem. Chem. Phys.*, 2005, **7**, 3297-3305.
57. K. Eichkorn, O. Treutler, H. Öhm, M. Häser and R. Ahlrichs, *Chem. Phys. Lett.*, 1995, **242**, 652-660.
58. K. Eichkorn, F. Weigend, O. Treutler and R. Ahlrichs, *Theor. Chem. Acc.*, 1997, **87**, 119-124.
59. E. D. Glendening, J. K. Badenhoop, A. E. Reed, J. E. Carpenter, J. A. Bohmann, C. M. Morales, C. R. Landis and F. Weinhold, *NBO 6.0*, 2013, , Theoretical Chemistry Institute, University of Wisconsin.
60. M. J. Frisch, G. W. Trucks, H. B. Schlegel, G. E. Scuseria, M. A. Robb, J. R. Cheeseman, G. Scalmani, V. Barone, B. Mennucci, G. A. Petersson, H. Nakatsuji, M. Caricato, X. Li, H. P. Hratchian, A. F. Izmaylov, J. Bloino, G. Zheng, J. L. Sonnenberg, M. Hada, M. Ehara, K. Toyota, R. Fukuda, J. Hasegawa, M. Ishida, T. Nakajima, Y. Honda, O. Kitao, H. Nakai, T. Vreven, J. A. Montgomery, J. E. Peralta, F. Ogliaro, M. Bearpark, J. J. Heyd, E. Brothers, K. N. Kudin, V. N. Staroverov, R. Kobayashi, J. Normand, K. Raghavachari, A. Rendell, J. C. Burant, S. S. Iyengar, J. Tomasi, M. Cossi, N. Rega, J. M. Millam, M. Klene, J. E. Knox, J. B. Cross, V. Bakken, C. Adamo, J. Jaramillo, R. Gomperts, R. E. Stratmann, O. Yazyev, A. J. Austin, R. Cammi, C. Pomelli, J. W. Ochterski, R. L. Martin, K. Morokuma, V. G. Zakrzewski, G. A. Voth, P. Salvador, J. J. Dannenberg, S. Dapprich, A. D. Daniels, Farkas, J. B. Foresman, J. V.

- Ortiz, J. Cioslowski and D. J. Fox, *Gaussian 09, Revision D.01*, 2013, Gaussian Inc., Wallingford CT.
61. G. A. Petersson, A. Bennett, T. G. Tensfeldt, M. A. Al-Laham and W. A. Shirley, *J. Chem. Phys.*, 1988, **89**, 2193-2218.
 62. G. A. Petersson and M. A. Al-Laham, *J. Chem. Phys.*, 1991, **94**, 6081-6090.
 63. A. Bergner, M. Dolg, W. Küchle, H. Stoll and H. Preuß, *Mol. Phys.*, 1993, **80**, 1431-1441.
 64. M. Dolg, U. Wedig, H. Stoll and H. Preuss, *J. Chem. Phys.*, 1987, **86**, 866-872.
 65. R. C. Cammarota, M. V. Vollmer, J. Xie, J. Ye, J. C. Linehan, S. A. Burgess, A. M. Appel, L. Gagliardi and C. C. Lu, *J. Am. Chem. Soc.*, 2017, **139**, 14244-14250.